PHYSIOLOGY 28: 172–189, 2013; doi:10.1152/physiol.00055.2012

Transduction of Voltage and Ca^{2+} Signals by Slo1 BK Channels

T. Hoshi,[1] A. Pantazis,[2] and R. Olcese[2,3,4]

[1]Department of Physiology, The University of Pennsylvania, Philadelphia, Pennsylvania; [2]Division of Molecular Medicine, Department of Anesthesiology, University of California, Los Angeles, California; [3]Brain Research Institute, University of California, Los Angeles, California; and [4]Cardiovascular Research Laboratories, University of California, Los Angeles, California

Large-conductance Ca^{2+}- and voltage-gated K^+ channels are activated by an increase in intracellular Ca^{2+} concentration and/or depolarization. The channel activation mechanism is well described by an allosteric model encompassing the gate, voltage sensors, and Ca^{2+} sensors, and the model is an excellent framework to understand the influences of auxiliary β and γ subunits and regulatory factors such as Mg^{2+}. Recent advances permit elucidation of structural correlates of the biophysical mechanism.

Large-conductance Ca^{2+}- and voltage-gated K^+ channels, also known as maxiK, BK, Slo1, $K_{Ca}1.1$, and KCNMA1 channels, open allosterically in response to an increase in intracellular Ca^{2+} concentration ($[Ca^{2+}]_i$), typically above 100 nM, and/or to membrane depolarization. The resulting net flux of K^+ according to its electrochemical gradient brings the membrane potential (V_m) closer to the equilibrium potential of K^+ (E_K), thus typically (but not necessarily; see Ref. 71) inhibiting cellular excitability in many cells types such as neurons, endocrine cells, and muscle cells. In other cells, such as solute-transporting epithelial cells in kidney, transport of K^+ through these high-conductance channels (≥100 pS, depending on K^+ concentrations) itself is the physiological outcome.

Physiological and pathophysiological contributions made by BK channels have been inferred by using pharmacological activators and inhibitors targeting BK channels and also by using mice with genetically altered BK channel complexes. Such studies have uncovered numerous but specific functional roles played by BK channels. For example, in some neurons, activation of BK channels contributes to fast after-hyperpolarization (100, 137), regulation of action potential firing frequency (47), and neurotransmitter release (60, 61). In smooth muscle cells, opening of BK channels promotes muscle relaxation (103), acting to protect against vascular hypertension (41, 102). Furthermore, neurovascular coupling to maintain proper cerebral circulation also involves BK channels (34). In endocrine and exocrine cells, BK channels control hormone release (117). Other physiological phenomena involving BK channels include skeletal muscle fatigue (75, 155), regulation of circadian rhythm (96), ethanol tolerance (27), and nociception (48). As expected from these diverse roles, a variety of pathological consequences may arise from BK channel dysfunction, including erectile dysfunction (166), incontinence (166), hypertension (18, 43), epilepsy (32), dyskinesia (32), seizure (16), asthma (136), and possibly obesity (68). Consequently, pharmaceutical agents targeting BK channels may prove therapeutically useful (33, 101). Undoubtedly, many more physiological and pathophysiological processes that critically depend on BK channels should be revealed in the near future.

The wide array of functions served by BK channels is made possible by their structural and functional diversity conferred by multiple mechanisms. For example, although only one gene codes for the pore-forming subunit (KCNMA1, Slo1), its transcript is extensively spliced to create a vastly large number of variant polypeptides (1, 36, 40, 141). Nearly 1,000 distinct full-length polypeptides may be theoretically available to form tetrameric BK channels in mice (125). Coassembly with the auxiliary subunits β1, β2, β3, β4, and leucine-rich repeat-containing proteins (LRRCs; γ subunits) also increases functional diversity by altering the channel's apparent sensitivity to Ca^{2+} and V_m as well as their kinetic properties including activation, deactivation, and in some cases conferring inactivation (11, 17, 156, 161, 165, 170, 176, 177). Participation in formation of macromolecular complexes with other signaling and ion channel proteins and post-translational modifications including phosphorylation, oxidation, and palmitoylation further expand the BK channel's functional repertoire (13, 79, 81, 135).

Central to the remarkable functional versatility of the BK channel is its allosteric activation involving Ca^{2+} and membrane depolarization as the primary physiological activators (121). Here, we will summarize recent advances in our understanding of how the BK channel transduces Ca^{2+} and voltage signals into opening of the ion conduction gate to regulate K^+ flux. The collective effort of many investigators utilizing different but complementary approaches has resulted in a clearer imagery of how membrane depolarization and intracellular Ca^{2+} activate the BK channel. However, despite the

1548-9213/13

availability of atomic structures of some regions of the channel, the picture is not yet crystal clear, and it lacks information on the dynamics of the structural rearrangements underlying BK channel operation and regulation by membrane potential, Ca^{2+}, and other signaling molecules. Additional efforts are clearly required to reveal the conformational dynamics of the channel to better understand the atomic and molecular bases of their function and regulation in health and disease.

Allosteric Activation by Ca^{2+} and Membrane Depolarization

Perhaps the most defining feature of the BK channel is its dualistic mechanism of activation involving Ca^{2+} and membrane depolarization. This is in contrast with small/intermediate-conductance Ca^{2+}-dependent K^+ (SK and IK) channels, which use a distinct Ca^{2+}-dependent activation mechanism involving calmodulin (CaM) with little voltage dependence (89, 127).

Early single-channel studies on native BK channels revealed the presence of multiple kinetically distinguishable closed and open states, and their dependence on Ca^{2+} (10, 87, 91–93, 97, 110, 143). The observation that depolarization in the virtual absence of Ca^{2+} robustly activates BK channels (30, 109, 126) in part led to the idea that the activation mechanism of the BK channel is allosteric in nature (28, 29, 52, 53, 123). This allosteric activation mechanism is perhaps best summarized by the model of Horrigan and Aldrich (HA model; FIGURE 1A) (52); each tetrameric BK channel complex (138) has one ion conduction gate, the opening and closing processes of which are influenced by the status of the Ca^{2+} sensors and voltage sensors, all in a reciprocal manner. That is, activation of the channel's voltage sensors by membrane depolarization increases the probability that the ion conduction gate is open (P_o), and, conversely, opening of the ion conduction gate allows the voltage sensors to activate more easily with depolarization. Similarly, binding of Ca^{2+} to the Ca^{2+} sensors of the channel increases the probability that the ion conduction gate is open, and opening of the gate in turn increases the affinity of the sensors to Ca^{2+}. Finally, voltage-sensor activation also increases the Ca^{2+} affinity, and Ca^{2+} binding to the sensors, in turn, promotes voltage-sensor activation. The end result is that the probability that the ion conduction gate is open increases with greater concentrations of $[Ca^{2+}]_i$ and/or depolarization (FIGURE 1B). Although the HA model omits some aspects of the channel gating (see Refs. 26, 130), the general concept is well supported by the experimental evidence, and the model has proven to be immensely useful as the conceptual framework to appreciate and analyze BK channel gating, for example, in studies of various auxiliary subunits, critical amino-acid residues, and modulators. Additionally, the formulation of the HA model largely reflects the physical organization of the BK channel protein, incorporating the consensus notion that proteins including the BK channel are made in a modular manner, whereby separate structural domains make distinct functional contributions, which are propagated through interdomain allosteric interactions. For more discussion on allosteric coupling in BK channels and other ion channels, interested readers are referred to Horrigan (50), Chowdhury and Chanda (25), and Sigg (142).

A few important corollaries of the allosteric gating mechanism are noteworthy. First, the BK channel does open without binding of Ca^{2+} or voltage-sensor activation, albeit at a very low probability (FIGURE 1B, BOTTOM) (53). Although the open probability of each channel may be small, one may observe occasional BK openings at rest when many BK channels are present in the membrane. Second, as implied above, a large increase in $[Ca^{2+}]_i$ without any depolarization can markedly increase P_o, and strong depolarization alone without any increase in $[Ca^{2+}]_i$ can increase P_o even to a near unity level. Third, because Ca^{2+} and/or depolarization facilitate opening, BK channel openings alone do not provide a simple and direct readout of $[Ca^{2+}]_i$ or V_m.

Snapshots of the BK Channel Structure

One functional BK channel is composed of four Slo1 polypeptides (138), each of which is typically ~1,100 residues long and most certainly forms multiple transmembrane segments connected by extracellular and intracellular loops (FIGURE 1C). In addition to the transmembrane helices S1–S6, which are found in voltage-dependent K^+ (K_V) channels, an additional transmembrane segment (S0) exists in Slo1 so that its NH_2 terminus faces the extracellular side (94, 160). The NH_2-terminal and transmembrane areas include only one-third of the total amino-acid residues, and the remainder makes up the cytoplasmic COOH-terminal domain, which is structurally organized into two tandem RCK (regulator of conductance for K^+) domains (RCK1 and RCK2). Despite their modest amino-acid sequence similarity (37), RCK1 and RCK2 exhibit a marked degree of three-dimensional structural similarity (172, 183, 184) (see below). It is conventionally thought that each RCK domain harbors its own micromolar-affinity Ca^{2+} sensing area: the RCK1 Ca^{2+} sensor (175, 185) and the RCK2 Ca^{2+} sensor (186), the latter of which is often referred to as the "Ca^{2+} bowl" (133). A short

stretch of ~20 residues connects the transmembrane helix S6 and RCK1 (S6-RCK1 linker), whereas ~100 or more residues bridge RCK1 and RCK2 (RCK1-RCK2 linker). Several splice variants that differ in the S6-RCK1 linker, the RCK1-RCK2 linker, and/or the distal COOH-terminal areas are known (125).

An experimentally determined atomic structure of the transmembrane domain of the BK channel is

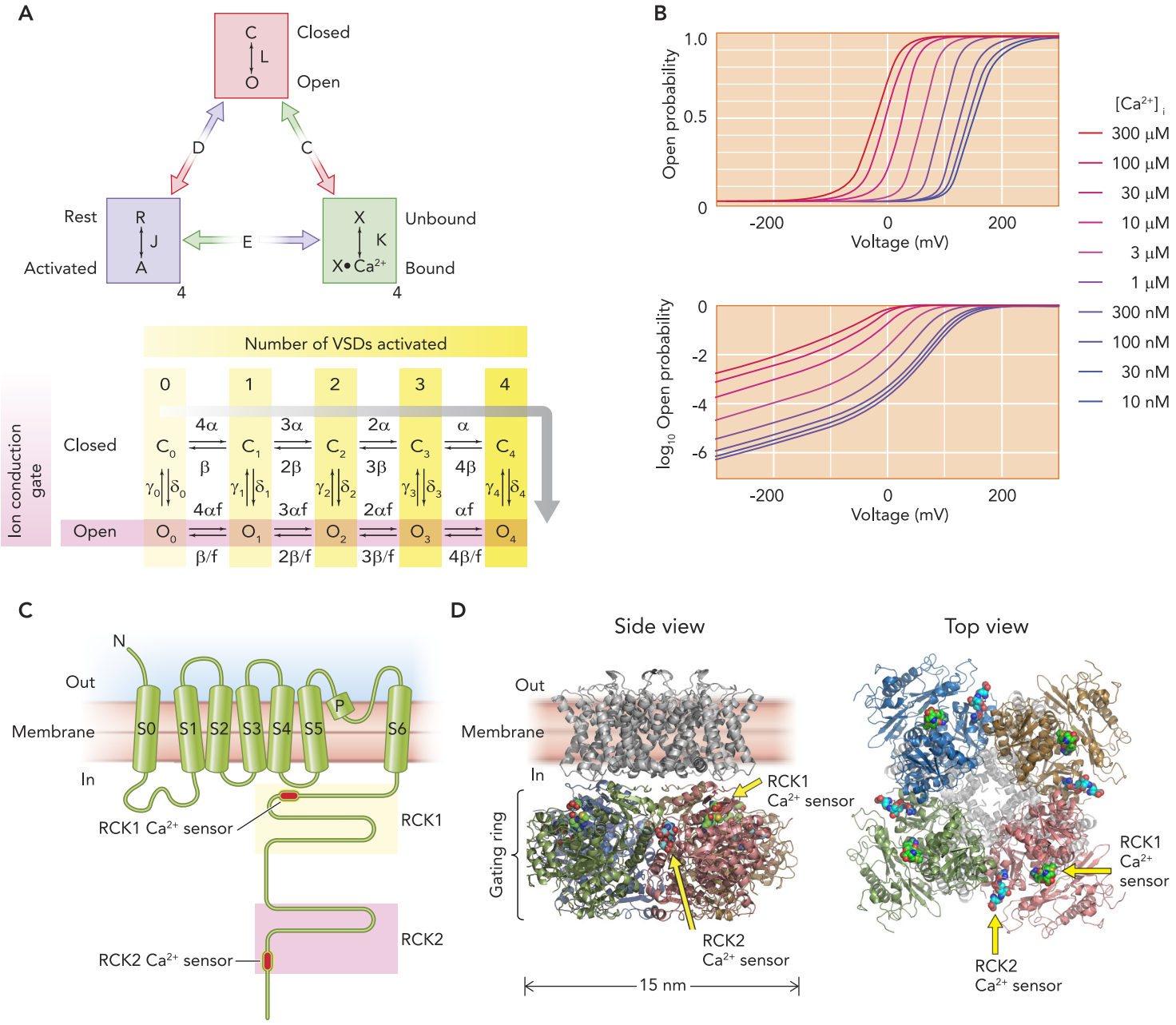

FIGURE 1. **The Horrigan and Aldrich model of gating**

A: the Horrigan and Aldrich (HA) model of gating of the Slo1 channel. L, J, and K are equilibrium constants describing the ion conduction gate, the voltage sensor, and the Ca^{2+} binding site, respectively. D, C, and E are allosteric interaction factors. For example, activation of one voltage sensor increases the value of L by D times, and activation of all four voltage sensors increases L by D^4. The kinetic model below the equilibrium model describes the channel behavior in the absence of Ca^{2+}. C_{0-4} are nonconducting states, and O_{0-4} are conducting states. The subscript number refers to the number of VSDs activated. For example, C_0 means that the ion conduction gate is closed and all four VSDs are at rest, and O_4 means that the ion conduction gate is open and all four VSDs are activated. α, β, γ_{0-4}, and δ_{0-4} are rate constants. $D = f^2$. The gray bent arrow indicates the likely activation pathway on moderate to large depolarization. *B*: voltage dependence of open probability of a typical human Slo1 channel predicted by the HA model on linear (*top*) and semi-logarithmic (*bottom*) scales with different $[Ca^{2+}]_i$. The graphs are for an illustrative purpose only. *C*: a schematic organization of one pore-forming Slo1 (α) polypeptide. Not drawn to scale. Of ~1,100 residues found in a typical Slo1 polypeptide, only ~320 residues are in the NH_2 terminus through S6. *D*: a plausible three-dimensional structural organization of a human Slo1 BK channel. The probable Ca^{2+} sensor locations are indicated by the two arrows. The transmembrane domain is a homology model based on a structure of a voltage-gated K^+ channel (PDB 2R9R), and the cytoplasmic domain is from PDB 3NAF obtained in the absence of added Ca^{2+} but without any Ca^{2+} chelator. The transmembrane segment S0 is not shown since the K_v channel lacks S0. The image was rendered in MacPyMol version 0.99. The spacing between the transmembrane domain and the cytoplasmic domain is only approximate. The transmembrane domain at *right* is made semi-transparent to better illustrate the gating ring domain.

not yet available. However, homology models have been constructed using the atomic structure of the $K_v1.2/2.1$ chimeric channel (85) as the template for the S1–S4 voltage sensor domain (VSD) and the bacterial Ca^{2+}-dependent channel MthK (66) for the S5-P-S6 pore domain (FIGURES 1D AND 4B) (184). Although the details of such homology models must be interpreted with extreme caution (e.g., Ref. 194), the overall size and shape of the transmembrane domain of the homology models are generally consistent with the image of the BK channel determined by electron cryomicroscopy (163); the transmembrane domain when viewed from the extracellular side has roughly a four-leaf clover shape with an overall diameter of ~10 nm. Four sets of S1–S4 protrude away from the central pore domain. Although the location of S0 cannot be inferred from the homology models, the cryomicroscopy study places it near the outer periphery of the protein (163). Furthermore, studies utilizing disulfide cross-linking of engineered cysteine residues (80) and collisional fluorescence quenching (112) place S0 close to S3 and S4.

In the tetrameric BK channel, four pairs of RCK1-RCK2 domains assemble to form a large torus-shaped cytoplasmic structure called the "gating ring," located intracellular to the transmembrane domain (FIGURE 1, C AND D) (172, 183, 184). The transmembrane and gating ring domains are proximal enough for close reciprocal functional interactions (130, 181). The exact distance and radial alignment between the transmembrane and cytoplasmic domains remain largely unknown, but some important preliminary information is now available from studies on the state-dependent effect of Mg^{2+} (see *Mg^{2+}-Dependent Activation* below) (181). Recently, atomic structures of the cytoplasmic gating ring at resolutions of 3–3.6 Å obtained with different concentrations of Ca^{2+} have been determined (172, 183, 184). The outer diameter of the gating ring is ~15 nm, ~50% larger than that of the transmembrane domain, and the diameter of the central star-shaped hole in the gating ring is ~4 nm. Both the RCK1 and RCK2 Ca^{2+} sensing sites are near the "top" of the gating ring domain, closer to the transmembrane domain (FIGURE 1D). Ca^{2+} binding to these sensors has been postulated to cause a conformational change in the gating ring, particularly around the regions facing the transmembrane domain, leading to an increase in the probability that the ion conduction gate is open (183). The S6-RCK1 linker, the RCK1-RCK2 linker, and the distal COOH terminus are not structured well enough under the crystallization conditions to be resolved. As with atomic structures of many other proteins, the direct relevance of the available atomic structures to the physiological operation of the BK channel remains to be established.

Molecular Correlates of the Components of the Allosteric Gating Mechanism

The Ion Conduction Gate

Functional and structural studies of various K^+ channels, including so-called two TM (transmembrane) voltage-independent K^+ channels and six TM voltage-dependent K_v channels, have shown that the primary ion conduction gate in these channels is formed by the four inner (S6) helices in the pore domain. When the four S6 helical bundles come together at the cytoplasmic end of the "cavity" or the "vestibule" and make a hydrophobic seal, the "gate" is closed. When the helical bundles splay outward, the gate is open and ions flow (see Ref. 65). In BK channels, however, multiple lines of evidence suggest that the cytoplasmic ends of the inner S6 helices do not significantly impede ion flow and that the primary ion conduction gate is located closer to the transmembrane selectivity filter region (24, 149, 152, 167, 194). For example, in contrast with the results obtained with K_v channels, the effectiveness of blocking molecules such as quaternary ammonium derivatives applied to the cytoplasmic side does not depend markedly on the ion conduction gate status (152, 167). Furthermore, Cys residues engineered at most positions in the BK S6 segment are very readily modified by a positively charged thiol modifier applied to the intracellular side even when the ion conduction gate is closed (194). A similar arrangement in which structural elements closer to the selectivity filter region serve as an ion conduction gate has been suggested for CNG channels allosterically activated by binding to cyclic nucleotides to the intracellular domain (35). Additionally, gating of TPRV1 channels activated by capsaicin and heat may also involve structural components near the selectivity filter (126). The placement of the primary ion conduction gate closer to the selectivity filter region may be generally preferred in those six TM channels modulated by various ligands. The physical mechanism by which the ion conduction gate of the BK channel regulates ion flow remains obscure. Because the amino-acid residues near/in the selectivity filter region probably constitute the ion conduction gate in the BK channel, it has been speculated that gating of the BK channel may resemble "C-type inactivation" transitions of K_v channels (167), which probably involve alterations in the selectivity filter region (56, 76).

The function of the ion conduction gate in the BK channel can be studied electrophysiologically

in isolation in the absence of the allosteric influences from activation of its Ca^{2+} sensors and voltage sensors (i.e., no Ca^{2+} at very negative potentials) (52, 53). Such measurements show that the gate function is weakly voltage dependent so that the open conformation is slightly more favored with depolarization, corresponding to an equivalent charge movement of ~0.3*e*. This small voltage dependence could be conferred by a subtle structural feature. A systematic mutagenesis study suggests that the weak voltage dependence of the gate may originate from S2 and/or S4 in the VSD (86). Even if the allosteric influence of voltage-sensor activation were to be removed, the gate would be ~1 million times more stable in the closed conformation in the absence of Ca^{2+} at 0 mV. Accordingly, the value of the equilibrium constant L_0 in the HA model is estimated to be $\sim 10^{-6}$, equivalent to the relative energetic stabilization of the closed conformation by ~8 kcal/mol (32.5 kJ/mol), not much more than the free energy of only a single hydrogen bond (5–30 kJ/mol). The gate equilibrium may be manipulated in a remarkable manner by mutations of select amino-acid residues in S6 halfway toward the cytoplasmic end in the amino-acid sequence (24, 171); however, it is not clear whether these residues actually form the gate that shuts off ion flow. In any case, the gate equilibrium is the ultimate effector of the two physiological activators of the channel, intracellular Ca^{2+} and membrane depolarization; Ca^{2+} binding and/or depolarization drastically shift the equilibrium toward the open conformation. Since allosteric interactions are reciprocal, the status of the ion conduction gate in turn influences the voltage and Ca^{2+} sensors (see below).

Voltage Sensors and Their Coupling to the Ion Conduction Gate

The closing and opening processes of the ion conduction gate in the pore domain are only modestly voltage dependent (52, 53), and the more robust voltage-dependent gating observed in the BK channel requires a separate domain specialized for voltage sensing. In the BK channel, the broadly conserved transmembrane helices S1–S4 (104) together with S0 constitute the voltage-sensor domain (VSD). Electrophysiological studies estimate that each VSD carries 0.6 voltage-sensing electronic charges or 2.4 charges/channel (51, 53), notably less than that in a typical K_v channel (up to ~16 charges/channel as summarized in Ref. 65). The smaller number of voltage-sensing charges may allow each BK channel to operate in a wide dynamic range of membrane potential and respond in a finely graded manner under diverse conditions. Furthermore, the small gating charge is a critical factor in the large shift in the half-activation voltage of P_o caused by increasing $[Ca^{2+}]_i$ (FIGURE 1B) (29).

In K_v channels, S4 is considered the principal component in voltage sensing because it harbors nearly all voltage-sensing positively charged residues (14, 21, 65, 145, 151, 154). At hyperpolarized potentials, the S4 positive charges are stabilized by negatively charged residues near the cytoplasmic side (114), resting or "down" state. Membrane depolarization favors an active or "up" conformation of this helix that repositions within the membrane electric field. Essentially, on depolarization, the S4 charges move outward, toward the extracellular side past an S2 hydrophobic residue where much of the membrane electrical field is narrowly focused, and then reestablish new electrostatic interactions with a different set of negatively charged residues in S2 and S3 at the extracellular side (65, 151, 159).

Although a similar mechanism may be operative in the BK channel, two notable differences are readily recognized. First, although the S4 segment of the BK channel typically contains four positively charged Arg residues (equivalent to R0, R2, R3, and R4 in K_v channels), only R4 (Arg213 in many mammalian Slo1) plays a measureable role in voltage sensing in the BK channel (86). R0, R2, and R3 may always reside out of the membrane electrical field in the extracellular compartment. Second, residues other than those in S4 contribute significantly to voltage sensing (86); thus the voltage-sensing charges in the BK channel are fewer and more "decentralized" than in the K_v channel. Specifically, S2 harbors two voltage-sensing residues, Asp153 and Arg167, and an additional voltage-sensing charge is located in S3 (Asp186) (86). This charge configuration results in complex relative motions occurring during voltage-dependent activation; fluorometry experiments with introduced collisional quenchers to report the relative rearrangements of assigned protein loci suggest that, upon depolarization, S4 diverges from S0, S1, and S2, while S2 approaches S1 (112, 113). Moreover, the motions of S2, brought about by the reorganization of its voltage-sensing charges in the membrane electrical field, enhance the voltage-sensing properties of S4 in a reciprocal and cooperative fashion because the neutralization of voltage-sensing charges in one segment impairs the voltage-dependent transition of the other (111). The cooperative interaction between the voltage-sensing S2 and S4 segments may be mediated in part through the water-filled crevices within the VSD (111), as better indicated in K_v channels (65, 85). The VSD crevices in the BK channel may appear and disappear during VSD activation and deactivation, altering the dielectric characteristics and the electric field profile, as suggested for

K_v-type channels (20, 21), thus contributing to the observed voltage-dependent cooperativity between S2 and S4 (111). Alternatively or additionally, the observed cooperativity between S2 and S4 may involve mechanical interactions between the two segments. Although multiple voltage-sensing residues may exist at dispersed locations within the VSD, the kinetics of BK gating currents elicited by brief depolarization appear well approximated by a single exponential (51, 144).

The aforementioned positively and negatively charged residues in S2, S3, and S4 together contribute to the overall voltage dependence of the BK channel, affecting the steepness of the curve relating V_m to the gate open probability [P_o(V) curve; FIGURE 1B]. It is important to note that the steepness of the P_o(V) curve is altered by many other variables besides the number of voltage-sensing charges, including the strength of coupling between the VSDs and the ion conduction gate (D in the HA model; FIGURE 1A).

S0, absent in K_v channels, plays an important role in functional assembly of Slo1 with its auxiliary β subunits (94, 160). In addition, S0 may also contribute to the VSD function because introduction of Trp residues to S0 alters the overall voltage dependence of channel activation (74). In agreement with this possibility, studies examining the efficiency of disulfide bond formation suggest that the extracellular end of S0 is located in close proximity of voltage-sensing S3 and S4 (82, 169). The proximity of S0 and S4 is also supported by the collisional quenching of small fluorophores conjugated to the extracellular flank of S0 (112).

In the absence of Ca^{2+} and when the ion conduction gate is closed, the VSD of the BK channel is typically much more stable in the resting or down conformation, and very large depolarization is required to fully drive the VSD to the activated or "up" conformation; a VSD half-activation voltage of ≥140 mV (J in the HA model; see FIGURE 1A) is commonly observed. The large depolarization required to activate the BK VSD may be contrasted with the observation that a typical K_v channel VSD is half-activated at approximately −45 mV. However, binding of Ca^{2+} to the BK channel dramatically biases the VSD equilibrium toward the activated conformation most probably through the sequential coupling of the Ca^{2+} sensor to the ion conduction gate (C in the HA model; FIGURE 1A) and then to the VSD (D in the HA model; FIGURE 1A), moving the half-activation voltage of the BK VSD to the more physiological direction. The direct coupling between the Ca^{2+} sensor and the VSD exists but it is much weaker (E in the HA model; FIGURE 1A) (52). For more details, interested readers are referred to Fig. 3 in Horrigan and Aldrich (52).

In the K_v channel, coupling between activation of the VSDs and opening of the ion conduction gate located at the S6 helical bundle (see above) is extremely tight such that activation of the VSDs almost always precedes opening of the ion conduction gate (131, 187): opening of the ion conduction gate is obligatorily coupled with activation of the VSD. As already indicated, this is not the case in the BK channel; the ion conduction gate may open frequently enough to measure unitary current openings at extreme negative membrane potentials (less than −100 mV) where the VSDs are mostly at rest (see FIGURE 1B, BOTTOM) (52). A similar nonobligatory mechanism likely exists for hyperpolarization-activated cyclic nucleotide-gated channels, which possess a large intracellular ligand-binding domain (19).

Activation of BK VSDs increases the probability that the ion conduction gate is open. According to the HA model, activation of one VSD increases the gate open probability by the allosteric strength factor D, which is numerically estimated to be ~20 (52). Therefore, with the assumption that the VSDs operate independently, activation of all four VSDs increases the gate open probability by 20^4 = 160,000. Experimentally, changes in coupling between VSD activation and the gate open probability are often seen as changes in steepness of P_o-V curves at the membrane potentials where some VSDs may be activated; the weaker the coupling strength (i.e., smaller D values), the shallower the P_o-V curve. However, it is important to note that a shallower P_o-V curve does not exclusively denote a decrease in D. Changes in other aspects of the HA model can also alter the steepness, such as a change in the number of voltage-sensing charges (e.g., Ref. 86). Changes in steepness of P_o-V curves have been observed with numerous mutations and modulators, some of which target the cytoplasmic gating ring domain (54), underscoring the intimate interaction between the transmembrane and cytoplasmic areas (181). Exactly how the events in the gating ring domain alter the coupling between the VSDs and the gate located in the transmembrane segments remains to be elucidated fully.

In K_v channels, the S4–S5 linker segment appears to work as a necessary linkage mechanism connecting the VSD movement to opening of the ion conduction gate at the cytoplasmic ends of the four S6 segments (65, 85). In the BK channel, the structural correlates of the VSD-gate coupling mechanism have not been clearly revealed. The S6-RCK1 linker in the BK channel connecting the transmembrane and the gating ring domain may contribute to the VSD-gate coupling process. Mutational shortening of this linker segment in the absence of Ca^{2+} shifts the P_o-V curve to the negative

direction, and lengthening of the linker shifts the curve to the positive direction without a noticeable change in their curve steepness (106). Whether these observations are caused by changes in coupling between the VSDs and the gate (i.e., D in the HA model), those in the VSD equilibrium (i.e., J in the HA model), and/or those in the intrinsic energetic stability of the ion conduction gate (i.e., L_0 in the HA model) remain to be studied in detail. Because the ion conduction gate of the BK channel may be located closer to the selectivity filter region, at least some of those residues located near/in the selectivity filter of the BK channel are probably capable of participating in the coupling process. For example, a Leu residue and a Phe residue located in the middle of S6, presumably cytoplasmic to the selectivity filter region, have been suggested to mediate the influences of VSD activation and Ca^{2+} binding on the ion conduction gate equilibrium (171).

Activation of the VSD is coupled reciprocally to opening of the ion conduction gate (D in the HA model; FIGURE 1) and to activation of the Ca^{2+} sensors directly (E in the HA model). It is also coupled indirectly to the Ca^{2+} sensors in a two-step manner through the ion conduction gate (D and C in the HA model). This coupling arrangement predicts that an increase in $[Ca^{2+}]_i$ without any change in V_m may induce a movement of the VSD. Indeed, in cut-open oocyte voltage-clamp fluorometry experiments, releasing Ca^{2+} intracellularly with the flash photolysis of caged-Ca^{2+} compounds induces a change in fluorescence consistent with a movement of the VSD (130).

Ca^{2+} Sensors and the Gating Ring

Changes in $[Ca^{2+}]_i$, typically in the range of 100 nM to 300 μM, steeply alter many aspects of gating of heterologously expressed Slo1 channels extremely rapidly without any need for coexpression of other proteins. For instance, single-channel P_o at 30 mV increases with $[Ca^{2+}]_i$ with a Hill coefficient of ~3.5 (122). The mean closed duration decreases with $[Ca^{2+}]_i$ with a Hill coefficient of ~3.5, whereas the mean open duration increases less steeply with a Hill coefficient of ~1 (122). Note that the estimated Hill coefficient value depends on the membrane potential (e.g., see Ref. 28), and the mechanistic usefulness of the Hill equation in explaining gating of the BK channel may be limited. The half-activation voltage ($V_{0.5}$) of macroscopic ionic currents may shift from >150 mV to ~0 mV when the Ca^{2+} sensors are fully activated by 300 μM of Ca^{2+} (FIGURE 1B) (52, 147). BK channels are further activated by greater concentrations (>1 mM) of intracellular divalent cations, especially Mg^{2+}, via the divalent cation sensors that are distinct from those that respond to micromolar levels of Ca^{2+} (139, 140, 175, 189, 191). Collectively, electrophysiological and mutagenesis results suggest that at least three functionally distinct divalent-cation sensors exist in the BK channel: *1*) the high-affinity RCK1 Ca^{2+} sensor in the cytoplasmic gating ring domain, *2*) the high-affinity RCK2 Ca^{2+} sensor (Ca^{2+} bowl) also in the cytoplasmic gating ring domain, and *3*) the low-affinity Mg^{2+} sensor formed by both the RCK1 domain and the transmembrane domain (FIGURE 1C) (63, 133, 140, 175, 189). See Hu et al. for an additional site (63). Under physiological conditions, BK channels are activated by Ca^{2+} binding to the Ca^{2+}-sensing sites in RCK1 and RCK2, the constituents of the gating ring structure. Thus the BK gating ring operates as a chemomechanical transducer, converting the free energy of Ca^{2+} binding into structural rearrangements. These Ca^{2+}-induced structural transitions are the subject of intense investigation, since they constitute the molecular basis by which this second messenger ultimately favors gate opening and VSD activation. Most of the studies on the Ca^{2+} sensors in the BK channel thus far utilized electrophysiological methods, and the results have been valuable. It must be recognized, however, that potentially confounding interpretational issues do exist. For example, the electrophysiological parameters estimated may not directly reflect the actual biophysical characteristics of the Ca^{2+} sensors, such as their affinities. Furthermore, estimation of Ca^{2+} binding parameters from electrophysiological measurements is not a trivial matter; it requires careful data fitting and simulations using a gating model of the channel such as the HA model or its derivatives (52, 130, 146). In addition, mutations that alter the overall Ca^{2+}-dependent activation of the BK channel may affect a Ca^{2+} sensor itself and/or the coupling mechanism bridging the sensor and its effector, interfering with straight-forward interpretations.

Ca^{2+} coordination by other proteins. Ca^{2+} ions, with an ionic radius of ~1 Å, interact with their binding sites in proteins through electrostatic interactions (116). A survey of crystallographic structures of Ca^{2+} binding proteins shows that a Ca^{2+} ion is coordinated by a variable number of electronegative oxygen atoms, typically six to eight, provided by the side chain carboxylate groups of aspartic and glutamic acids, backbone carboxyl groups, and nearby water molecules (69). Ligation of Ca^{2+} is sometimes described as "loose" with a typical Ca-O distance of 2.3–2.6 Å (116). The coordination arrangement is well illustrated in binding of Ca^{2+} in CaM (FIGURE 2A), perhaps the best-known "EF hand" Ca^{2+}-binding protein. A short loop segment (seven residues), very closely flanked by two helical segments, surrounds the bound Ca^{2+} ion. The oxygen atoms of the side chains of Asp20, Asp22, Asp24, and Glu31 as well as the

backbone carbonyl oxygen atom of Thr26 act as the ligands. In particular, Glu31 is a bidentate ligand in that both of the two side chain oxygen atoms interact with the Ca^{2+} ion. The ion is also stabilized by one water molecule so that the total coordination number is 7.

RCK2 (Ca^{2+} bowl) sensor. Inspection of the amino-acid sequence of Slo1 (1) revealed the presence of five consecutive negatively charged Asp residues (Ca^{2+} bowl) toward the COOH terminus of the protein and led to the idea that these residues may coordinate Ca^{2+} and act as a Ca^{2+} sensor linked to opening of the channel (133). The Ca^{2+} bowl sensor or the RCK2 Ca^{2+} sensor is located in a longer loop segment (~16–20 residues) of the RCK2 domain near the subunit-subunit interface where Gln889, Asp892, Asp895, and Asp 897 (bidentate), neighboring residues in the primary structure, coordinate the central Ca^{2+} ion (FIGURE 2B). The oxygen atoms, forming a coordination sphere of ~4.1 Å in diameter, are provided by the backbone carbonyl groups of Gln889 and Asp 892, and by the side chains of Asp895 and Asp897. Up to three water molecules may be bound to the ion so that the coordination number totals to 6–8. In the absence of bound Ca^{2+} (PDB ID 3NAF), the aforementioned Ca^{2+}-coordinating oxygen atoms are much more dispersed in space (>8 Å apart), presumably because the electronegative oxygen atoms repel each other. It is these structural changes induced by Ca^{2+} coordination starting in the Ca^{2+} sensors that lead to experimentally detectable changes in the whole gating ring assembly (see below), culminating in dramatic stabilization of the open conformation of the ion conduction gate near the selectivity filter. The conformational changes in the purified RCK2 domain protein by physiological levels of Ca^{2+} have been detected by circular dichroism (186). The apparent Ca^{2+} dissociation constants for the RCK2 Ca^{2+} sensor when the ion conduction gate is closed (K_c) and open (K_o) have been estimated electrophysiologically to be ~3.1 and ~0.88 μM, respectively (146). The ratio K_c/K_o = 3.5 represents the allosteric interaction factor C in the HA model (FIGURE 1A), and the difference K_o-K_c represents the allosteric influence of the ion conduction gate on each RCK2 Ca^{2+} sensor, corresponding to ~3 kJ/mol. This translates into a 3.5-fold (K_c/K_o) increase in the probability that the ion conduction gate is open when one RCK2 sensor coordinates a Ca^{2+} ion or an ~150-fold (3.5^4) increase in P_o when all four RCK2 sensors are Ca^{2+} bound (146).

Neutralization of the Ca^{2+}-coordinating residues within the RCK2 sensor partially impaired the negative shift of the $P_o(V)$ curve by Ca^{2+} and binding of Ca^{2+} to the COOH-terminal protein fragments (8, 15, 133), suggesting that the Ca^{2+} bowl segment is a Ca^{2+} sensor. The mutations did not, however, fully obliterate the Ca^{2+} sensitivity in either electrophysiological (133) or biochemical assays (8, 15, 64), hinting the existence of a second Ca^{2+} sensor, the presence of which was later corroborated (see below) (175).

RCK1 sensor. The atomic structures of the isolated gating ring domain solved in the presence of mM levels of Ca^{2+} (PDB IDs 3MT5 and 3U6N) (183, 184), greater than those required to fully activate wild-type BK channels through the high-affinity Ca^{2+} sensors, do not show any Ca^{2+} bound to the RCK1 domain. The reasons for the lack of bound Ca^{2+} in the structures are unclear. The structural integrity of the RCK1 Ca^{2+} sensor may require the transmembrane segments, and the crystallization conditions [e.g., low pH (184)] may have interfered with Ca^{2+} binding. Nevertheless, other lines of evidence strongly suggest the existence of a Ca^{2+}

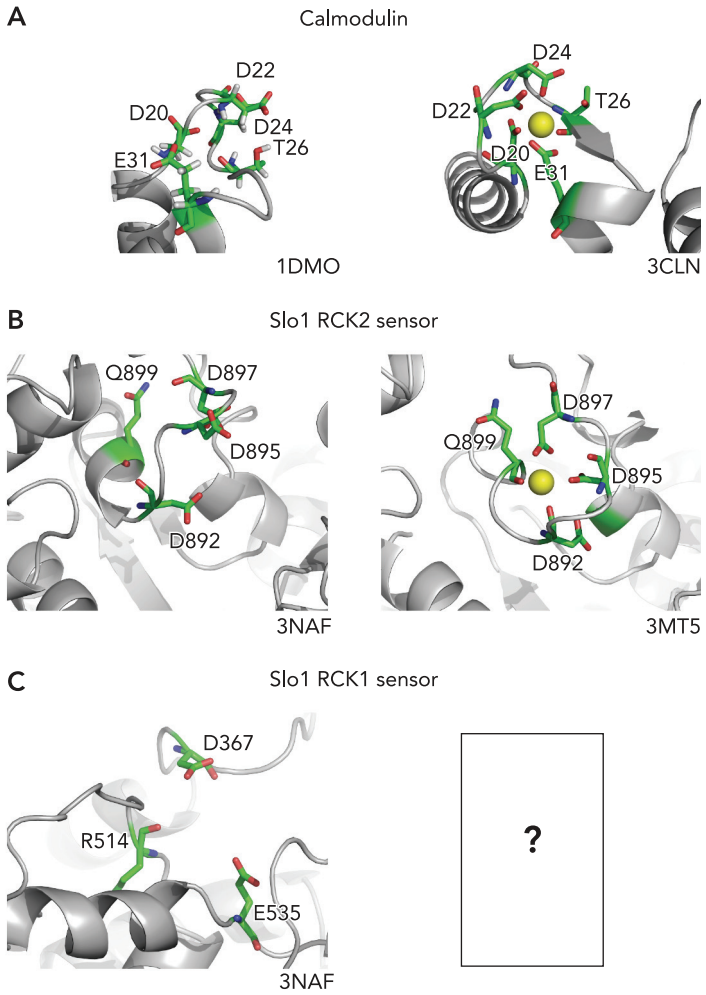

FIGURE 2. **Ca^{2+} coordination**
Ca^{2+} coordination in calmodulin (*A*), the Slo1 RCK2 sensor (*B*), and the Slo1 RCK1 sensor (*C*). For each, the Ca^{2+}-free apo structure is shown at *left* and the Ca^{2+}-bound structure is shown at *right*. The image was rendered in MacPyMol version 0.99. The Ca^{2+}-ligating residues are shown using sticks. Ca^{2+}: yellow sphere; carbon: green; nitrogen: blue; oxygen: red. Water molecules participate in Ca^{2+} coordination, but they are not shown.

sensor in the RCK1 domain (9, 175, 185, 189). The consensus is that structural groups from at least three amino-acid residues, markedly noncontiguous in the primary structure, unlike in CaM or the RCK2 Ca^{2+} sensor, participate in coordination of a Ca^{2+} ion: Asp367 side chain (175, 189), the Glu535 side chain (190), and Arg514 backbone (190). A few water molecules are likely complexed with the Ca^{2+} ion in the RCK1 sensor. In addition, Met513 may participate in formation of the RCK1 sensor (9); however, the structural details are not obvious because the carbonyl group of Met513 projects away from Asp367, Glu535, and Arg514 in the atomic structures (PDB IDs 3NAF, 3MT5, and 3U6N). The Ca^{2+} coordination arrangement of the RCK1 sensor may be proven to be different from those in the RCK2 sensor and CaM. Interestingly, the probable Ca^{2+}-coordinating oxygen atoms of the RCK1 sensor are spatially further apart and more dispersed in the atomic structures of the gating ring domain, with Ca^{2+} bound to the RCK2 sensors (3MT5 and 3U6N) than in that without any Ca^{2+} bound (3NAF). This observation may be consistent with the suggestion that negative cooperativity may exist between the RCK1 and RCK2 sensors (Refs. 130, 146; but see Ref. 119). The critical role of the RCK1 sensor in the Ca^{2+}-dependent activation mechanism has been highlighted by the discovery that a mutation of Asp369 (D369G), near the Ca^{2+}-coordinating Asp367 in the RCK1 Ca^{2+} sensor, is associated with human epilepsy and paroxysmal movement disorder (32).

The apparent Ca^{2+} dissociation constants of the RCK1 sensor when the ion conduction gate is closed and open (K_c and K_o) are electrophysiologically estimated to be ~23 and 4.9 μM, respectively (146). Comparing the estimated affinity values of the RCK1 and RCK2 sensors, greater concentrations of Ca^{2+} are typically required to activate the RCK1 sensor than the RCK2 sensor. However, the allosteric coupling between the RCK1 sensor and the ion conduction gate is stronger than that between the RCK2 sensor and the gate (146). The difference in apparent Ca^{2+} affinity of the RCK1 sensor when the gate is closed and open ($K_c - K_o$) is greater, corresponding to ~3.8 kJ/mol, and the ratio K_c/K_o (4.7) is also greater for the RCK1 sensor. Thus the ion conduction gate is ~4.7 times more likely to be in the open conformation for each Ca^{2+} bound to the RCK1 Ca^{2+} sensor: ~487-fold (4.7^4) increase in P_o when all four RCK1 sensors are Ca^{2+} bound (146).

Ca^{2+}-induced conformational changes in the cytoplasmic gating ring domain. Studies using bacterial Ca^{2+}-activated but voltage-independent 2TM K^+ channels suggested that Ca^{2+}-induced structural changes in the cytoplasmic gating ring domain accompany the opening and closing processes of the ion conduction gate; "expansion" of the gating ring domain promotes opening of the gate (31, 66). In particular, an outward radial expansion of the gating ring may pull the ion conduction gate open (31, 66). A similar conformational change was speculated to occur in the BK channel (67). The atomic structures of the BK gating ring domain obtained under different conditions [no added Ca^{2+} but without any Ca^{2+} chelator (3NAF) vs. Ca^{2+}-rich (3MT5 and 3U6N)] reveal that they are discernibly different, suggesting that the gating ring domain motion does accompany opening of the ion conduction gate. In particular, Ca^{2+} binding to the RCK2 sensors may change the conformation of the gating ring so that the layer of the gating ring domain immediately juxtapositional to the transmembrane segments opens up like the petals of a flower (FIGURE 3) (183). Presumably, it is the free energy change associated with these conformational changes in the cytoplasmic gating ring domain that ultimately promotes opening of the ion conduction gate near the transmembrane selectivity filter. It is important to remember, however, that the physiological relevance of these atomic structures remains to be established. Furthermore, the preferred allosteric "communication pathway," "allosteric trajectory" (124), or "conformational wave" (44) between the gating ring domain and the ion conduction gate, if it exists (49), is yet to be elucidated. The idea that the gating ring domain undergoes a measurable Ca^{2+}-induced conformational change has been corroborated by spectroscopic studies of the isolated tetrameric gating ring domain in solution (64). Based on the diffusional properties of particles in solution, dynamic light scattering measurements show that Ca^{2+} binding causes a reversible reduction of the hydrodynamic radius of the gating ring domain; the protein assumes a shape with a greater rate of diffusion (64). Furthermore, clear changes in both steady-state and time-resolved fluorescence of native Trp residues reporting their local environments are detected (64). Thus these solution-based biochemical studies have revealed that the gating ring possesses a dynamic structure capable of reversibly undergoing shape alterations in response to changes in $[Ca^{2+}]_i$. Unfortunately, these changes cannot be readily related to the available atomic structures because of the significant differences in the experimental conditions utilized in the studies.

Are the RCK1 and RCK2 Ca^{2+} sensors functionally similar? Both the RCK1 and RCK2 Ca^{2+} sensor sites are located near the outer radial edge of the gating ring domain (FIGURE 1). The two sensors appear to face toward the internal surface of the plasma membrane and are ~25 Å apart in each subunit. The exact manner by which the two sensors

in one subunit functionally interact to regulate P_o remains to be established (119, 130, 146). As noted earlier, the two sensors do differ in their electrophysiologically estimated apparent Ca^{2+} affinity values and their coupling to opening of the gate; Ca^{2+} binds to the RCK2 sensor more tightly at negative membrane potentials (146). Additionally, Ca^{2+} binding to the RCK1 sensor but not to the RCK2 sensor is estimated to be voltage dependent, becoming tighter with depolarization (146), most probably indirectly through the interaction between the RCK1 Ca^{2+} sensor and the ion conduction gate. Furthermore, gate opening kinetics of the channel may be more intimately linked to Ca^{2+} binding to the RCK2 sensor, whereas the closing kinetics may be coupled more strongly to Ca^{2+} binding to the RCK1 sensor (189). The allosteric consequences of Ca^{2+} binding to the two sensors were further investigated by optically tracking the activation of the VSD using cut-open oocyte voltage-clamp fluorometry while releasing Ca^{2+} intracellularly with the flash photolysis of caged-Ca^{2+} compounds (130). Ca^{2+} binding to the gating ring at constant V_m facilitated VSD activation, as predicted by the allosteric coupling pathways among the gate, the VSDs, and the Ca^{2+} sensors. Interestingly, this Ca^{2+}-induced movement of the VSD requires an intact Ca^{2+} bowl area.

Ca^{2+} is the physiological ligand for both the RCK1 and RCK2 sensors in all likelihood. Yet, the two sensors are capable of binding other divalent cations, at least under experimental conditions. The RCK2 sensor preferentially coordinates Ba^{2+}, Sr^{2+}, and Ca^{2+}, whereas the RCK1 sensor coordinates Sr^{2+}, Ca^{2+}, and Cd^{2+} (195). It is noteworthy that Ba^{2+}, a well known pore blocker of many K^+ channels including BK channels, binds preferentially to the RCK2 sensor and promotes opening of the ion conduction gate, albeit with a weaker affinity and a smaller efficacy (195). The weaker electrophysiological effect of Ba^{2+} on gate opening compared with Ca^{2+} may involve a smaller and/or different conformational change by Ba^{2+} in the cytoplasmic gating ring domain. This possibility is consistent with the finding that, unlike Ca^{2+}, Ba^{2+} does not markedly alter the native Trp fluorescence from the isolated gating ring protein in solution (64). The differential effects of Ba^{2+} on the RCK1 and RCK2 sensors suggest that the two sensors coordinate divalent cations, including Ca^{2+}, in distinct fashions, perhaps with the RCK2 Ca^{2+} bowl sensor preferring those divalent cations with larger ionic radii (195), and their coupling to the ion conduction gate is also different.

The RCK1 sensor, but not the RCK2 sensor, is involved in activation of BK channels by low intracellular pH (59). H^+ promotes opening of the BK channel with an EC_{50} of pH ~6.5, and the stimulatory effect diminishes with increasing concentrations of Ca^{2+} or Mg^{2+}; H^+ may induce the same conformational changes as those caused by Ca^{2+} and/or Mg^{2+} (6, 57). One of the residues critical for the H^+ action is His365 (59), whose imidazole side chain is found in close contact with the side chain of Asp367 (3NAF) or of Arg514 (3MT5 and 3U6N), both of which likely coordinate Ca^{2+} in the RCK1 sensor (see above). Protonation/deprotonation of His365 may therefore transmit the same information to the ion conduction gate as that by ligation of Ca^{2+} by the RCK1 sensor. Additionally, His365 may ligate Zn^{2+}, a potential

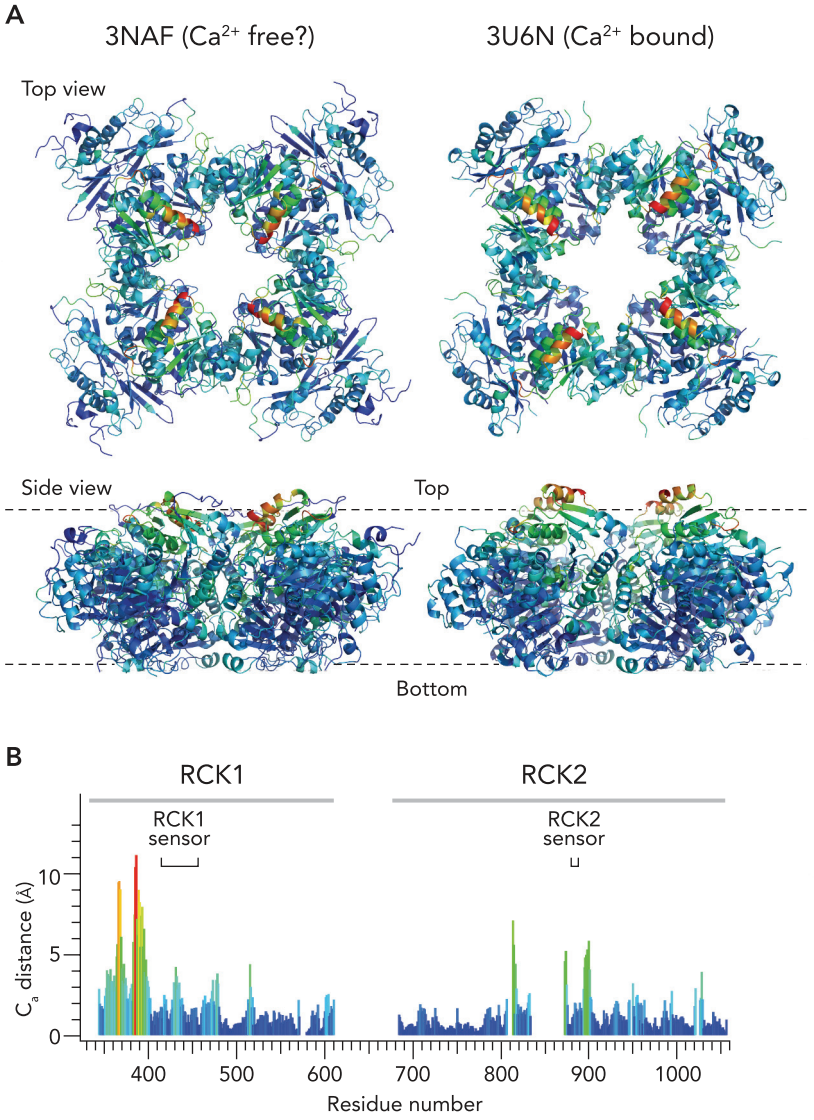

FIGURE 3. **Potential changes in the conformation of the cytoplasmic gating ring domain by Ca^{2+}**
A: atomic structures of the human Slo1 gating ring domain (PDB 3NAF) obtained without Ca^{2+} (but without any Ca^{2+} chelator) and of the zebrafish Slo1 gating ring domain with Ca^{2+} bound to the RCK2 sensor but not to the RCK1 sensor (PDB 3U6N) are compared. The colors represent the distances between the corresponding α carbons in the two structures. Red: 11 Å; purple: 0 Å. *B*: distances between the α carbons of the corresponding residues in 3NAF and 3U6N. The residue numbers represent those in human Slo1 as in 3NAF. The structures were analyzed and rendered in MacPyMol version 0.99.

physiological signaling molecule (38), and promote BK channel activation (58).

Mg^{2+}-Dependent Activation

Elevations of $[Ca^{2+}]_i$ to 100 nM to 100 μM, sensed by the RCK1 and RCK2 sensors (see above), increase the probability of gate opening in the BK channel. Greater concentrations of Ca^{2+}as well as of select divalent cations such as Mg^{2+} (>1 mM) produce additional activation. This "low-affinity" response is often referred to as Mg^{2+}-dependent activation because the underlying mechanism has been studied primarily with Mg^{2+} (139, 140, 175, 189, 191). The low-affinity (Mg^{2+}-dependent) activation and the high-affinity (Ca^{2+}-dependent) activation processes are electrophysiologically different, reflecting their distinct molecular mechanisms (55, 180). For example, in the absence of VSD activation at very negative voltages, Ca^{2+} is capable of increasing P_o, reflecting the direct allosteric coupling of the Ca^{2+} sensors and the ion conduction gate (see FIGURE 1). However, under such a condition, Mg^{2+} (10 mM) is without effect, and the Mg^{2+}-dependent increase in P_o becomes evident only at more depolarized voltages at which VSD activation is significant (55). Furthermore, it is not the membrane depolarization itself that is required for Mg^{2+} to increase P_o but rather VSD activation (23, 55).

In aqueous solution, Mg^{2+}, with a small ionic radius of 0.65 Å, is surrounded by six water molecules arranged in an octahedral configuration (116). In proteins, oxygen atoms from amino acids, in a monodentate fashion, and nearby water molecules coordinate Mg^{2+} so that the total coordination number is 6, forming a coordination sphere smaller than that for Ca^{2+} (116). In the BK channel, the Mg^{2+}-coordinating oxygen atoms are provided by the amino-acid residues from both the transmembrane domain containing the VSD and the intracellular RCK1 domain. More specifically, Asp99 in the intracellular S0–S1 loop, Asn172 in the S2–S3 loop, and Glu374 and Glu399 in the RCK1 domain are probable Mg^{2+} ligands (140, 175, 179, 180), leaving room for two water molecules to participate.

The Mg^{2+} coordination mechanism in the BK channel, where the oxygen atoms provided by the residues from the VSDs and those from the cytoplasmic gating ring domain sandwiching Mg^{2+} between them, nicely explains the observation that the Mg^{2+} action requires VSD activation (23, 55). Studies utilizing gating current measurements show that Mg^{2+} coordinated in the interdomain space and the voltage-sensing residue Arg213 in S4 lead to an electrostatic repulsion between them, stabilizing the activated or "up" state of the VSD when the ion conduction gate is open (55, 62, 180). Mg^{2+} may be thus considered as a modulator of the allosteric coupling strength between the VSD and the ion conduction gate ("D" in the HA model; FIGURE 1) (55). Collectively, the information gained from studies of Mg^{2+}-dependent activation of BK channels has provided valuable insights and implications about the structural dynamics of the BK channel. For example, because the Mg-O distance is typically ~2.0–2.1 Å (116), the Mg^{2+} coordination arrangement described above suggests that the VSDs and the RCK1 domains are within a few Angstroms of each other under certain conditions, for instance, when Mg^{2+} ions are bound. The state-dependent apposition of the transmembrane VSDs and the cytoplasmic gating ring domain may also explain the observations that some BK channel modulators, such as free heme (150), bind to the gating ring domain yet influence aspects of the VSD function (54).

The physiological role of Mg^{2+}-dependent activation of the BK channel is yet to be fully revealed. Some pathophysiological relevance is suggested by the finding that ethanol, at the concentrations induced by binge drinking, lowers the intracellular Mg^{2+} concentration (3, 4). The lack of tonic Mg^{2+}-dependent activation of BK channels in vascular smooth muscle cells may contribute to ethanol-induced cerebrovasospasm and ischemia (4). It may be noted, however, that ethanol exerts multiple effects on BK channels including a direct activation action (83, 84).

Contributions by Auxiliary Subunits

Native BK channels are extremely diverse in their pharmacological and gating characteristics. For example, some neuronal BK channels are potently inhibited by the peptide neurotoxin charybdotoxin at ≤10 nM, whereas others are virtually unaffected (120). Some BK channels open very frequently at negative resting potentials, whereas others require appreciable depolarization (39, 153). Some BK currents also show prominent inactivation (173). This remarkable diversity is conferred in part by coassembly of pore-forming Slo1 (α) subunits with various auxiliary subunits (170, 176). To date, two vertebrate families of auxiliary subunits, β and γ, have been identified (FIGURE 4A) (170, 176). Four β-subunits, β1 (coded by the gene KCNMB1), β2 (KCNMB2), β3 (KCNMB3), and β4 (KCNMB4), are known (11, 17, 156, 161, 165, 170, 174). The β3 transcript is alternatively spliced to produce at least four different variants (β3a, b, c, and d) (156). The γ-subunit family has only recently been discovered and may potentially represent a large group of leucine-rich repeat-containing (LRRC) proteins (2, 176, 177) that are structurally and functionally distinct from β-subunits. Expression of

both β- and γ-subunits is tissue dependent, albeit overlapping and not mutually exclusive. Although skeletal muscle cells do not have an appreciable level of expression of any β, smooth muscle cells predominantly express Slo1 + β1 (18, 148). Slo1 + β4 channels are readily found in neuronal and endocrine cells (11, 17). Inclusion of β1-subunits can dramatically modify pharmacological sensitivities of the channel complexes (70, 90, 158), including their toxin sensitivity (95). The β-subunits are also capable of regulating functional consequences of mutations and modulatory phenomena originating within the pore-forming subunit Slo1 (77, 128, 157, 182). For example, the functional impact of the epilepsy-/dyskinesia-causing mutation D369G depends on the β-subunit (77). Changes in the auxiliary subunit composition of BK channel complexes may be involved in some diseases states (5, 192). Invertebrates such as *Drosophila* do not appear to possess β-like subunits, but instead they maintain their own sets of proteins that interact with the pore-forming subunits in a different manner (132).

β-Subunits

Atomic structures of β-subunits are not yet known; however, available studies collectively show that the β-subunit is a glycosylated two transmembrane (TM1 and TM2) protein, 170–280 residues in length, with its NH_2 and COOH termini facing the intracellular side (FIGURE 4A) (72, 73). The amino-acid sequences in TM1 and TM2 of the four β-subunits show a relatively high degree of similarity, whereas they are more diverse in the NH_2 terminus, the extracellular linker, and the COOH terminus. Up to four β-subunits are present within a tetrameric Slo1 complex (73, 164). Multiple lines of evidence suggest that, at the extracellular side, TM1 of one β-subunit faces S1 and S2, components of the VSD (see above), of one Slo1 subunit, and TM2 faces S0 of a neighboring Slo1 subunit (FIGURE 4B) (80, 98, 168, 169).

Inclusion of β-subunits in BK complexes markedly alters their gating characteristics. Perhaps the most readily observable modification is the inactivation process induced by β2- and some β3-subunits. Although ionic currents through the channels made of pore-forming Slo1 subunits alone do not exhibit any inactivation, coexpression with β2 or select β3 induces inactivation mediated by the NH_2 terminus of the auxiliary subunit (161, 174). It should be noted, however, that this β2-/β3-induced inactivation in BK channels is in many ways distinct from N-type inactivation in Shaker/K_v channels (42, 129) and is not associated with immobilization of the voltage-sensing charges (42, 129).

Activation and deactivation kinetics of ionic currents through Slo1 + β1, Slo1 + β2ΔN (a deletion in the NH_2 terminus of β2 to remove inactivation), and Slo1 + β4 at low $[Ca^{2+}]_i$ are markedly slower than those through Slo1 without any auxiliary subunits (Slo1). In addition, functional consequences of Ca^{2+} binding in Slo1 + β1, Slo1 + β2ΔN, and Slo1 + β4 channels are greater than that of Slo1 alone (7, 105, 107, 147, 162). In Slo1 alone, saturating concentrations of Ca^{2+} (100–300 μM) shift the half-activation voltage of macroscopic ionic currents from ≥150 mV to <0 mV (FIGURE 1B). With β1, the shift is ~30% greater, bringing the half-activation voltage to −100 mV or less (7, 107, 147). With β2ΔN, the half-activation voltage is also −100 mV or less (107) and with β4 it is about −50 mV (162). These gating changes and others by β1, β2ΔN, and β4 have been subjected to analyses to estimate the values of the parameters of the HA model (7, 107, 162). Unfortunately, however, the analysis results are somewhat divergent. One potential reason for the perplexing findings may be that the experimental results failed to constrain the parameter values sufficiently. Yet another is that, despite the similarity in the overall structural organization noted above, different β-subunits may exert very distinct modulatory influences (7, 107, 162). In human Slo1 + human β1, human Slo1 + human β2ΔN, and mouse Slo1 + mouse β4, the closed conformation of the ion conduction gate is >10 times more stable than that in Slo1 alone; the value of L_0 in the HA model is appreciably smaller (but see Ref. 7). In these Slo1 + β complexes, noticeably fewer openings are observed at negative

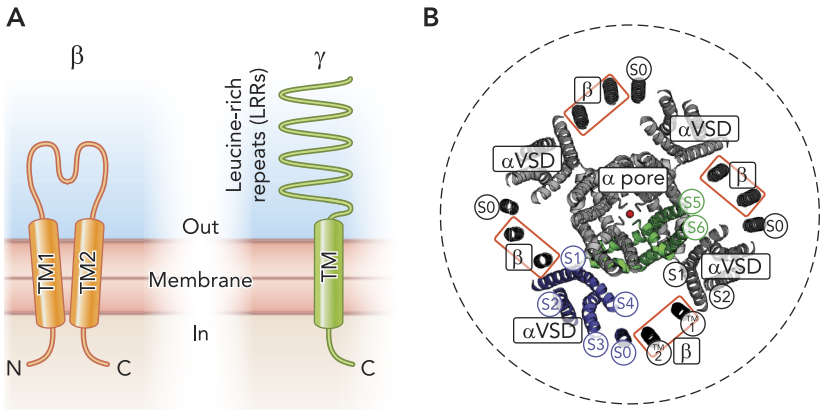

FIGURE 4. **Auxiliary subunits of Slo1**

A: schematic organizations of prototypical β and γ (LRRC) subunits. Not drawn to scale. *B*: probable relative positions of Slo1 and β subunits viewed from the extracellular side. The Slo1 transmembrane structure is based on a homology model. Each Slo1 (α) subunit consists of seven transmembrane helices, of which S0–S4 make up a voltage-sensing domain (VSD, green), whereas S5–S6 (green) contribute to the central, the K^+-selective pore (a conducting K^+ is shown in red). Auxiliary β subunits possess two transmembrane (TM) helices (black), of which TM2 associates with α subunit S0, whereas TM1 associates with S1 of a neighboring α subunit (80). S0, TM1, and TM2 were constructed as ideal α helices and positioned according to Liu et al. (80). The dashed circle represents the size of the cytoplasmic gating ring domain (~15 nm in diameter).

voltages without Ca^{2+} than in Slo1 alone (107, 162). In addition, in the presence of β1, β2ΔN, or β4, the activated state of the VSD is stabilized by various degrees (7, 26, 107, 129, 162). More focused studies, examining subsets of the transitions within the HA model, suggest that the presence of β1 alters the two Ca^{2+} sensors of the channel differentially (147). As noted earlier, the RCK1 Ca^{2+} sensor has a lower affinity than the RCK2 Ca^{2+} bowl sensor, but its coupling to the ion conduction gate is approximately two times stronger. With β1, the K_d value of the RCK1 Ca^{2+} sensor when the gate is open (K_o) decreases by fourfold (i.e., affinity is higher) to a level similar to that of the RCK2 Ca^{2+} bowl sensor and increases the coupling strength (C in the HA model) by fourfold. The RCK2 Ca^{2+} bowl sensor is less affected by β1; the K_d value when the gate is closed (K_c) increases by approximately two to threefold and the enhancement in coupling strength is approximately twofold. Therefore, the RCK1 Ca^{2+} sensor contributes more prominently to the increase in the overall Ca^{2+} sensitivity seen in Slo1 + β1 channels. A qualitatively similar increase in coupling between the Ca^{2+} sensors and the ion conduction gate is reported for Slo1 + β4 (162). The characteristic slowing of the activation and deactivation kinetics of ionic currents at low $[Ca^{2+}]_i$ when β1, β2ΔN, or β4 is present is not accompanied by appreciable slowing of "on" or "off" gating charge movements, which predominantly reflect the kinetics of the VSD (7, 26). Therefore, the slower ionic currents in Slo1 + β1, Slo1 + β2ΔN, and Slo1 + β4 are probably caused by changes in the kinetics of the ion conduction gate.

γ-Subunits

Frequent BK channel openings at negative resting membrane potentials were once interpreted to signify a high level of $[Ca^{2+}]_i$. This conventional thinking was shattered by the recordings from rodent cochlear hair cells (153) and also from prostate and breast cancer cells (39); some BK channels do open without much Ca^{2+} at negative voltages. In the aforementioned cancer cells, this characteristic is conferred by LRRC26, the founding member of the γ-subunit family (177). At the plasma membrane surface, LRRC26 (γ1) possess a single transmembrane segment with a large extracellular NH_2-terminal domain containing five leucine-rich repeat motifs (FIGURE 1A) (177). Overexpression of LRRC26 (γ1) shifts the half-activation voltage of macroscopic ionic currents without Ca^{2+} from >160 to ~0 mV, similar to that caused by 100 μM $[Ca^{2+}]_i$! This remarkable shift in the overall voltage dependence of activation is caused by a 20-fold increase in the strength of coupling between the VSD and the ion conduction gate (D in the HA model). LRRC26 (γ1) is only one of several LRRC proteins that could function as BK channel auxiliary subunits in a tissue-dependent manner (2, 176); different LRRC proteins appear to influence the BK channel function to different degrees (176). The stoichiometry between Slo1 and γ-subunits in native channel complexes is not known. LRRC proteins are capable of interacting with other ion channels; for example, LRRC52 markedly modifies functional properties of Slo3 channels (178), which are activated by alkalization and are critical for fertility (134).

Physicochemical Mechanisms of Regulation by β- and γ-Subunits

Multiple regions of Slo1 and β-subunits have been implicated in proper functional coassembly between them: Slo1 transmembrane domain (78, 94, 99, 160), Slo1 cytoplasmic gating ring domain (78, 118), β extracellular linker (46), and β NH_2- and COOH-terminal intracellular regions (108, 188). However, the exact physicochemical mechanisms by which the β-subunits induce the various functional changes remain unresolved. The probable location of the β-subunit [between two adjacent VSDs (FIGURE 4B)] suggests that the β-subunit may influence the VSD energetics (26) through direct interactions and/or indirectly via membrane lipids. How the behavior of the ion conduction gate, most likely located near the selectivity filter within the central pore domain, is influenced by the β-subunits near the periphery of the channel complex is unclear. The physicochemical mechanism underlying the remarkable effect of LRRC26 (γ1) is also obscure. The functional effects of β1 and LRRC26 (γ1) compete, suggesting that LRRC26 (γ1) subunit positions itself between two VSDs near the central pore domain, like β-subunits, to alter the coupling between the VSD and the gate (177).

Where Does Ca^{2+} Come From?

Many BK channels exist as components of macromolecular signaling complexes so that the channels transduce local signals, whether they be Ca^{2+} or other messengers. One of the best known examples is found in vascular smooth muscle cells. Whereas global increases in $[Ca^{2+}]_i$ induce muscle contraction, local and discrete increases in $[Ca^{2+}]_i$ mediated by ryanodine receptor channels in the sarcoplasmic reticulum promote vasorelaxation by activating Slo1 + β1 channels (18). The local $[Ca^{2+}]_i$ near the BK channels in arterial smooth muscle cells has been estimated to be ≥10 μM during contraction (115, 196), near or above the estimated K_d values of the Ca^{2+} sensors in Slo1 + β1 (147).

Ca^{2+} influx through plasma membrane ion channels also activates nearby BK channels. Differential effects of the slow Ca^{2+} chelator EGTA and the fast Ca^{2+} chelator BAPTA (197) on neuronal action potential repolarization suggest that the distance between the voltage-gated Ca^{2+} channel pore and the BK channel Ca^{2+} sensor is only ~13 nm (100). This distance is surprisingly small because the radius of the transmembrane domain of the BK channel is probably ~5 nm and that of the voltage-gated Ca^{2+} channel is expected to be similar, leaving only a few nanometers between the two channels (12). The Ca^{2+} ions entering through voltage-gated Ca^{2+} channels do not travel far to bind to BK channel complexes. An observation in line with this concept was reported earlier in hippocampal neurons: a small unitary inward Ca^{2+} channel opening was suggested to be followed immediately by an outward BK channel opening (88). Consistent with these functional results, multiple types of voltage-gated Ca^{2+} channels (L-type $Ca_V1.2$, N-type Ca_V 2.2, P/Q-type $Ca_V2.1$, and potentially T-type $Ca_V3.2$) (12, 13, 22, 45) appear capable of forming close physical interactions with BK channel complexes. Additionally, BK channels form complexes with NMDA glutamate receptors (193) and also with IP_3 receptor channels (193).

Concluding Remarks

The BK channel is an exemplar model of allosteric regulation of ion channel proteins. The modular components of the BK channel are each capable of activation in response to a specific energy type: the membrane potential and chemical potential of Ca^{2+} and other ligands. The VSD and gating ring are sensors and transducers that detect and propagate the signals to the "active site" of the protein, namely the ion selectivity filter and its associated gate. These remarkable features, together with the unusually large unitary conductance, allow the channel to participate in numerous physiological functions. ■

We thank the members of the Hoshi and Olcese laboratories and Dr. F. Horrigan for critical comments on the manuscript.

The authors' laboratories are supported in part by research grants from National Institute of General Medical Sciences Grants R01 GM-057654 (T. Hoshi) and R01 GM-082289 (R. Olcese), the German Research Foundation Grant FOR 1738 (T. Hoshi), and American Heart Association Beginning Grant in Aid 12BGIA10560007 (A. Pantazis).

No conflicts of interest, financial or otherwise, are declared by the author(s).

Author contributions: T.H., A.P., and R.O. conception and design of research; T.H., A.P., and R.O. performed experiments; T.H., A.P., and R.O. analyzed data; T.H., A.P., and R.O. interpreted results of experiments; T.H., A.P., and R.O. prepared figures; T.H., A.P., and R.O. drafted manuscript; T.H., A.P., and R.O. edited and revised manuscript; T.H., A.P., and R.O. approved final version of manuscript.

References

1. Adelman JP, Shen KZ, Kavanaugh MP, Warren RA, Wu YN, Lagrutta A, Bond CT, North RA. Calcium-activated potassium channels expressed from cloned complementary DNAs. *Neuron* 9: 209–216, 1992.
2. Almassy J, Begenisich T. The LRRC26 protein selectively alters the efficacy of BK channel activators. *Mol Pharmacol* 81: 21–30, 2012.
3. Altura BM, Altura BT, Gupta RK. Alcohol intoxication results in rapid loss in free magnesium in brain and disturbances in brain bioenergetics: relation to cerebrovasospasm, alcohol-induced strokes, and barbiturate anesthesia-induced deaths. *Magnes Trace Elem* 10: 122–135, 1991.
4. Altura BM, Zhang A, Cheng TP, Altura BT. Ethanol promotes rapid depletion of intracellular free Mg in cerebral vascular smooth muscle cells: possible relation to alcohol-induced behavioral and stroke-like effects. *Alcohol* 10: 563–566, 1993.
5. Amberg GC, Bonev AD, Rossow CF, Nelson MT, Santana LF. Modulation of the molecular composition of large conductance, Ca^{2+} activated K^+ channels in vascular smooth muscle during hypertension. *J Clin Invest* 112: 717–724, 2003.
6. Avdonin V, Tang XD, Hoshi T. Stimulatory action of internal protons on Slo1 BK channels. *Biophys J* 84: 2969–2980, 2003.
7. Bao L, Cox DH. Gating and ionic currents reveal how the BK_{Ca} channel's Ca^{2+} sensitivity is enhanced by its β1 subunit. *J Gen Physiol* 126: 393–412, 2005.
8. Bao L, Kaldany C, Holmstrand EC, Cox DH. Mapping the BKCa channel's "Ca^{2+} bowl": side-chains essential for Ca^{2+} sensing. *J Gen Physiol* 123: 475–489, 2004.
9. Bao L, Rapin AM, Holmstrand EC, Cox DH. Elimination of the BK_{Ca} channel's high-affinity Ca^{2+} sensitivity. *J Gen Physiol* 120: 173–189, 2002.
10. Barrett JN, Magleby KL, Pallotta BS. Properties of single calcium-activated potassium channels in cultured rat muscle. *J Physiol* 1982: 211–230, 1982.
11. Behrens R, Nolting A, Reimann F, Schwarz M, Waldschutz R, Pongs O. hKCNMB3 and hKCNMB4, cloning and characterization of two members of the large-conductance calcium-activated potassium channel β subunit family. *FEBS Lett* 474: 99–106, 2000.
12. Berkefeld H, Fakler B, Schulte U. Ca^{2+}-activated K^+ channels: from protein complexes to function. *Physiol Rev* 90: 1437–1459, 2010.
13. Berkefeld H, Sailer CA, Bildl W, Rohde V, Thumfart JO, Eble S, Klugbauer N, Reisinger E, Bischofberger J, Oliver D, Knaus HG, Schulte U, Fakler B. BK_{Ca}-Cav channel complexes mediate rapid and localized Ca^{2+}-activated K^+ signaling. *Science* 314: 615–620, 2006.
14. Bezanilla F. How membrane proteins sense voltage. *Nat Rev Mol Cell Biol* 9: 323–332, 2008.
15. Bian S, Favre I, Moczydlowski E. Ca^{2+}-binding activity of a COOH-terminal fragment of the *Drosophila* BK channel involved in Ca^{2+}-dependent activation. *Proc Natl Acad Sci USA* 98: 4776–4781, 2001.
16. Brenner R, Chen QH, Vilaythong A, Toney GM, Noebels JL, Aldrich RW. BK channel β4 subunit reduces dentate gyrus excitability and protects against temporal lobe seizures. *Nat Neurosci* 8: 1752–1759, 2005.
17. Brenner R, Jegla TJ, Wickenden A, Liu Y, Aldrich RW. Cloning and functional characterization of novel large conductance calcium-activated potassium channel β subunits, hKCNMB3 and hKCNMB4. *J Biol Chem* 275: 6453–6461, 2000.
18. Brenner R, Perez GJ, Bonev AD, Eckman DM, Kosek JC, Wiler SW, Patterson AJ, Nelson MT, Aldrich RW. Vasoregulation by the β1 subunit of the calcium-activated potassium channel. *Nature* 407: 870–876, 2000.
19. Bruening-Wright A, Elinder F, Larsson HP. Kinetic relationship between the voltage sensor and the activation gate in spHCN channels. *J Gen Physiol* 130: 71–81, 2007.

20. Cha A, Bezanilla F. Characterizing voltage-dependent conformational changes in the Shaker K^+ channel with fluorescence. *Neuron* 19: 1127–1140, 1997.

21. Chanda B, Bezanilla F. A common pathway for charge transport through voltage-sensing domains. *Neuron* 57: 345–351, 2008.

22. Chen CC, Lamping KG, Nuno DW, Barresi R, Prouty SJ, Lavoie JL, Cribbs LL, England SK, Sigmund CD, Weiss RM, Williamson RA, Hill JA, Campbell KP. Abnormal coronary function in mice deficient in α_{1H} T-type Ca^{2+} channels. *Science* 302: 1416–1418, 2003.

23. Chen RS, Geng Y, Magleby KL. Mg^{2+} binding to open and closed states can activate BK channels provided that the voltage sensors are elevated. *J Gen Physiol* 138: 593–607, 2011.

24. Chen X, Aldrich RW. Charge substitution for a deep-pore residue reveals structural dynamics during BK channel gating. *J Gen Physiol* 138: 137–154, 2011.

25. Chowdhury S, Chanda B. Free-energy relationships in ion channels activated by voltage and ligand. *J Gen Physiol* 141: 11–28, 2013.

26. Contreras GF, Neely A, Alvarez O, Gonzalez C, Latorre R. Modulation of BK channel voltage gating by different auxiliary β subunits. *Proc Natl Acad Sci USA* 109: 18991–18996, 2012.

27. Cowmeadow RB, Krishnan HR, Ghezzi A, Al'Hasan YM, Wang YZ, Atkinson NS. Ethanol tolerance caused by slowpoke induction in *Drosophila*. *Alcohol Clin Exp Res* 30: 745–753, 2006.

28. Cox DH, Cui J, Aldrich RW. Allosteric gating of a large conductance Ca-activated K^+ channel. *J Gen Physiol* 110: 257–281, 1997.

29. Cui J, Aldrich RW. Allosteric linkage between voltage and Ca^{2+}-dependent activation of BK-type mslo1 K^+ channels. *Biochemistry* 39: 15612–15619, 2000.

30. Cui J, Cox DH, Aldrich RW. Intrinsic voltage dependence and Ca^{2+} regulation of mslo large conductance Ca-activated K^+ channels. *J Gen Physiol* 109: 647–673, 1997.

31. Dong J, Shi N, Berke I, Chen L, Jiang Y. Structures of the MthK RCK domain and the effect of Ca^{2+} on gating ring stability. *J Biol Chem* 280: 41716–41724, 2005.

32. Du W, Bautista JF, Yang H, Diez-Sampedro A, You SA, Wang L, Kotagal P, Luders HO, Shi J, Cui J, Richerson GB, Wang QK. Calcium-sensitive potassium channelopathy in human epilepsy and paroxysmal movement disorder. *Nat Genet* 37: 733–738, 2005.

33. Eichhorn B, Dobrev D. Vascular large conductance calcium-activated potassium channels: functional role and therapeutic potential. *Naunyn Schmiedebergs Arch Pharmacol* 376: 145–155, 2007.

34. Filosa JA, Bonev AD, Straub SV, Meredith AL, Wilkerson MK, Aldrich RW, Nelson MT. Local potassium signaling couples neuronal activity to vasodilation in the brain. *Nat Neurosci* 9: 1397–1403, 2006.

35. Flynn GE, Zagotta WN. Conformational changes in S6 coupled to the opening of cyclic nucleotide-gated channels. *Neuron* 30: 689–698, 2001.

36. Fodor AA, Aldrich RW. Convergent evolution of alternative splices at domain boundaries of the BK channel. *Annu Rev Physiol* 71: 19–36, 2009.

37. Fodor AA, Aldrich RW. Statistical limits to the identification of ion channel domains by sequence similarity. *J Gen Physiol* 127: 755–766, 2006.

38. Frederickson CJ, Koh JY, Bush AI. The neurobiology of zinc in health and disease. *Nat Rev Neurosci* 6: 449–462, 2005.

39. Gessner G, Schönherr R, Soom M, Hansel A, Asim M, Baniahmad A, Derst C, Hoshi T, Heinemann SH. BK_{Ca} channels activating at resting potential without calcium in LNCaP prostate cancer cells. *J Membr Biol* 208: 229–240, 2006.

40. Glauser DA, Johnson BE, Aldrich RW, Goodman MB. Intragenic alternative splicing coordination is essential for *Caenorhabditis elegans slo-1* gene function. *Proc Natl Acad Sci USA* 108: 20790–20795, 2011.

41. Gollasch M, Tank J, Luft FC, Jordan J, Maass P, Krasko C, Sharma AM, Busjahn A, Bahring S. The BK channel β1 subunit gene is associated with human baroreflex and blood pressure regulation. *J Hypertens* 20: 927–933, 2002.

42. Gonzalez-Perez V, Zeng XH, Henzler-Wildman K, Lingle CJ. Stereospecific binding of a disordered peptide segment mediates BK channel inactivation. *Nature* 485: 133–136, 2012.

43. Grimm PR, Sansom SC. BK channels and a new form of hypertension. *Kidney Int*: 956–962, 2010.

44. Grosman C, Zhou M, Auerbach A. Mapping the conformational wave of acetylcholine receptor channel gating. *Nature* 403: 773–776, 2000.

45. Grunnet M, Kaufmann WA. Coassembly of big conductance Ca^{2+}-activated K^+ channels and L-type voltage-gated Ca^{2+} channels in rat brain. *J Biol Chem* 279: 36445–36453, 2004.

46. Gruslova A, Semenov I, Wang B. An extracellular domain of the accessory β1 subunit is required for modulating BK channel voltage sensor and gate. *J Gen Physiol* 139: 57–67, 2011.

47. Gu N, Vervaeke K, Storm JF. BK potassium channels facilitate high-frequency firing and cause early spike frequency adaptation in rat CA1 hippocampal pyramidal cells. *J Physiol* 580: 859–882, 2007.

48. Hendrich J, Alvarez P, Chen X, Levine JD. GDNF induces mechanical hyperalgesia in muscle by reducing I_{BK} in isolectin B4-positive nociceptors. *Neuroscience* 219: 204–213, 2012.

49. Hilser VJ, Wrabl JO, Motlagh HN. Structural and energetic basis of allostery. *Annu Rev Biophys* 41: 585–609, 2012.

50. Horrigan FT. Conformational coupling in BK potassium channels. *J Gen Physiol* 140: 625–634, 2012.

51. Horrigan FT, Aldrich RW. Allosteric voltage gating of potassium channels II. mslo channel gating charge movement in the absence of Ca^{2+}. *J Gen Physiol* 114: 305–336, 1999.

52. Horrigan FT, Aldrich RW. Coupling between voltage sensor activation, Ca^{2+} binding and channel opening in large conductance (BK) potassium channels. *J Gen Physiol* 120: 267–305, 2002.

53. Horrigan FT, Cui J, Aldrich RW. Allosteric voltage gating of potassium channels I. mslo ionic currents in the absence of Ca^{2+}. *J Gen Physiol* 114: 277–304, 1999.

54. Horrigan FT, Heinemann SH, Hoshi T. Heme regulates allosteric activation of the Slo1 BK channel. *J Gen Physiol* 126: 7–21, 2005.

55. Horrigan FT, Ma Z. Mg^{2+} enhances voltage sensor/gate coupling in BK channels. *J Gen Physiol* 131: 13–32, 2008.

56. Hoshi T, Armstrong CM. C-type inactivation of voltage-gated K^+ channels: pore constriction or dilation? *J Gen Physiol*, 2013.

57. Hou S, Horrigan FT, Xu R, Heinemann SH, Hoshi T. Comparative effects of H^+ and Ca^{2+} on large-conductance Ca^{2+}- and voltage-gated Slo1 K^+ channels. *Channels (Austin)* 3: 249–258, 2009.

58. Hou S, Vigeland LE, Zhang G, Xu R, Li M, Heinemann SH, Hoshi T. Zn^{2+} activates large-conductance Ca^{2+} -activated K^+ channel via an intracellular domain. *J Biol Chem* 285: 6434–6442, 2010.

59. Hou S, Xu R, Heinemann SH, Hoshi T. Reciprocal regulation of the Ca^{2+} and H^+ sensitivity in the SLO1 BK channel conferred by the RCK1 domain. *Nat Struct Mol Biol* 15: 403–410, 2008.

60. Hu H, Shao LR, Chavoshy S, Gu N, Trieb M, Behrens R, Laake P, Pongs O, Knaus HG, Ottersen OP, Storm JF. Presynaptic Ca^{2+}-activated K^+ channels in glutamatergic hippocampal terminals and their role in spike repolarization and regulation of transmitter release. *J Neurosci* 21: 9585–9597, 2001.

61. Hu H, Shao LR, Chavoshy S, Gu N, Trieb M, Behrens R, Laake P, Pongs O, Knaus HG, Ottersen OP, Storm JF. Presynaptic Ca^{2+}-activated K^+ channels in glutamatergic hippocampal terminals and their role in spike repolarization and regulation of transmitter release. *J Neurosci* 21: 9585–9597, 2001.

62. Hu L, Shi J, Ma Z, Krishnamoorthy G, Sieling F, Zhang G, Horrigan FT, Cui J. Participation of the S4 voltage sensor in the Mg^{2+}-dependent activation of large conductance (BK) K^+ channels. *Proc Natl Acad Sci USA* 100: 10488–10493, 2003.

63. Hu L, Yang H, Shi J, Cui J. Effects of multiple metal binding sites on calcium and magnesium-dependent activation of BK channels. *J Gen Physiol* 127: 35–50, 2006.

64. Javaherian AD, Yusifov T, Pantazis A, Franklin S, Gandhi CS, Olcese R. Metal-driven operation of thehuman large-conductance voltage- and Ca^{2+}-dependent potassium channel (BK) gating ring apparatus. *J Biol Chem* 286: 20701–20709, 2011.

65. Jensen MØ, Jogini V, Borhani DW, Leffler AE, Dror RO, Shaw DE. Mechanism of voltage gating in potassium channels. *Science* 336: 229–233, 2012.

66. Jiang Y, Lee A, Chen J, Cadene M, Chait BT, MacKinnon R. Crystal structure and mechanism of a calcium-gated potassium channel. *Nature* 417: 515–522, 2002.

67. Jiang Y, Pico A, Cadene M, Chait BT, MacKinnon R. Structure of the RCK domain from the *E. coli* K^+ channel and demonstration of its presence in the human BK channel. *Neuron* 29: 593–601, 2001.

68. Jiao H, Arner P, Hoffstedt J, Brodin D, Dubern B, Czernichow S, van't Hooft F, Axelsson T, Pedersen O, Hansen T, Sorensen TI, Hebebrand J, Kere J, Dahlman-Wright K, Hamsten A, Clement K, Dahlman I. Genome wide association study identifies KCNMA1 contributing to human obesity. *BMC Medical Genomics* 4: 51, 2011.

69. Katz AK, Glusker JP, Beebe SA, Bock CW. Calcium ion coordination: a comparison with that of beryllium, magnesium, and zinc. *J Am Chem Soc* 118: 5752–5763, 1996.

70. King JT, Lovell PV, Rishniw M, Kotlikoff MI, Zeeman ML, McCobb DP. β2 and β4 subunits of BK channels confer differential sensitivity to acute modulation by steroid hormones. *J Neurophysiol* 95: 2878–2888, 2006.

71. Klyachko VA, Ahern GP, Jackson MB. cGMP-mediated facilitation in nerve terminals by enhancement of the spike afterhyperpolarization. *Neuron* 31: 1015–1025, 2001.

72. Knaus HG, Eberhart A, Kaczorowski GJ, Garcia ML. Covalent attachment of charybdotoxin to the β-subunit of the high conductance Ca^{2+}-activated K^+ channel. Identification of the site of incorporation and implications for channel topology. *J Biol Chem* 269: 23336–23341, 1994.

73. Knaus HG, Garcia-Calvo M, Kaczorowski GJ, Garcia ML. Subunit composition of the high conductance calcium-activated potassium channel from smooth muscle, a representative of the mSlo and slowpoke family of potassium channels. *J Biol Chem* 269: 3921–3924, 1994.

74. Koval OM, Fan Y, Rothberg BS. A role for the S0 transmembrane segment in voltage-dependent gating of BK channels. *J Gen Physiol* 129: 209–220, 2007.

75. Kristensen M, Hansen T, Juel C. Membrane proteins involved in potassium shifts during muscle activity and fatigue. *Am J Physiol Regul Integr Comp Physiol* 290: R766–R772, 2006.

76. Kurata HT, Fedida D. A structural interpretation of voltage-gated potassium channel inactivation. *Prog Biophys Mol Biol* 92: 185–208, 2006.

77. Lee US, Cui J. β subunit-specific modulations of BK channel function by a mutation associated with epilepsy and dyskinesia. *J Physiol* 587: 1481–1498, 2009.

78. Lee US, Shi J, Cui J. Modulation of BK channel gating by the β2 subunit involves both membrane-spanning and cytoplasmic domains of Slo1. *J Neurosci* 30: 16170–16179, 2010.

79. Li M, Tanaka Y, Alioua A, Wu Y, Lu R, Kundu P, Sanchez-Pastor E, Marijic J, Stefani E, Toro L. Thromboxane A2 receptor and MaxiK-channel intimate interaction supports channel trans-inhibition independent of G-protein activation. *Proc Natl Acad Sci USA* 107: 19096–19101, 2010.

80. Liu G, Niu X, Wu RS, Chudasama N, Yao Y, Jin X, Weinberg R, Zakharov SI, Motoike H, Marx SO, Karlin A. Location of modulatory β subunits in BK potassium channels. *J Gen Physiol* 135: 449–459, 2010.

81. Liu G, Shi J, Yang L, Cao L, Park SM, Cui J, Marx SO. Assembly of a Ca^{2+}-dependent BK channel signaling complex by binding to β2 adrenergic receptor. *EMBO J* 23: 2196–2205, 2004.

82. Liu G, Zakharov SI, Yang L, Deng SX, Landry DW, Karlin A, Marx SO. Position and role of the BK channel alpha subunit S0 helix inferred from disulfide crosslinking. *J Gen Physiol* 131: 537–548, 2008.

83. Liu J, Asuncion-Chin M, Liu P, Dopico AM. CaM kinase II phosphorylation of slo Thr107 regulates activity and ethanol responses of BK channels. *Nat Neurosci* 9: 41–49, 2006.

84. Liu J, Bukiya A, Kuntamallappanavar G, Singh A, Dopico A. Distinct sensitivity of Slo1 channel proteins to ethanol. *Mol Pharmacol* 83: 235–244, 2012.

85. Long SB, Tao X, Campbell EB, MacKinnon R. Atomic structure of a voltage-dependent K^+ channel in a lipid membrane-like environment. *Nature* 450: 376–382, 2007.

86. Ma Z, Lou XJ, Horrigan FT. Role of charged residues in the S1–S4 voltage sensor of BK channels. *J Gen Physiol* 127: 309–328, 2006.

87. Magleby KL, Pallotta BS. Calcium dependence of open and shut interval distributions from calcium-activated potassium channels in cultured rat muscle. *J Physiol* 344: 585–604, 1983.

88. Marrion NV, Tavalin SJ. Selective activation of Ca^{2+}-activated K^+ channels by co-localized Ca^{2+} channels in hippocampal neurons. *Nature* 395: 900–905, 1998.

89. Maylie J, Bond CT, Herson PS, Lee WS, Adelman JP. Small conductance Ca^{2+}-activated K^+ channels and calmodulin. *J Physiol* 554: 255–261, 2004.

90. McManus OB, Helms LM, Pallanck L, Ganetzky B, Swanson R, Leonard RJ. Functional role of the β subunit of high conductance calcium-activated potassium channels. *Neuron* 14: 645–650, 1995.

91. McManus OB, Magleby KL. Accounting for the Ca^{2+}-dependent kinetics of single large-conductance Ca^{2+}-activated K^+ channels in rat skeletal muscle. *J Physiol* 443: 739–777, 1991.

92. McManus OB, Magleby KL. Kinetic states and modes of single large-conductance calcium-activated potassium channels in cultured rat skeletal muscle. *J Physiol* 402: 79–120, 1988.

93. McManus OB, Magleby KL. Kinetic time constants independent of previous single-channel activity suggest Markov gating for a large conductance Ca-activated K channel. *J Gen Physiol* 94: 1037–1070, 1989.

94. Meera P, Wallner M, Song M, Toro L. Large conductance voltage- and calcium-dependent K^+ channel, a distinct member of voltage-dependent ion channels with seven N-terminal transmembrane segments (S0–S6), an extracellular N terminus, and an intracellular (S9–S10) C terminus. *Proc Natl Acad Sci USA* 94: 14066–14071, 1997.

95. Meera P, Wallner M, Toro L. A neuronal β subunit (KCNMB4) makes the large conductance, voltage- and Ca^{2+}-activated K^+ channel resistant to charybdotoxin and iberiotoxin. *Proc Natl Acad Sci USA* 97: 5562–5567, 2000.

96. Meredith AL, Wiler SW, Miller BH, Takahashi JS, Fodor AA, Ruby NF, Aldrich RW. BK calcium-activated potassium channels regulate circadian behavioral rhythms and pacemaker output. *Nat Neurosci* 9: 1041–1049, 2006.

97. Methfessel C, Boheim G. The gating of single calcium-dependent potassium channels is described by an activation/blockade mechanism. *Biophys Struct Mech* 9: 35–60, 1982.

98. Morera FJ, Alioua A, Kundu P, Salazar M, Gonzalez C, Martinez AD, Stefani E, Toro L, Latorre R. The first transmembrane domain (TM1) of β2-subunit binds to the transmembrane domain S1 of α-subunit in BK potassium channels. *FEBS Lett* 586: 2287–2293, 2012.

99. Morrow JP, Zakharov SI, Liu G, Yang L, Sok AJ, Marx SO. Defining the BK channel domains required for β1-subunit modulation. *Proc Natl Acad Sci USA* 103: 5096–5101, 2006.

100. Muller A, Kukley M, Uebachs M, Beck H, Dietrich D. Nanodomains of single Ca^{2+} channels contribute to action potential repolarization in cortical neurons. *J Neurosci* 27: 483–495, 2007.

101. Nardi A, Olesen SP. BK channel modulators: a comprehensive overview. *Curr Med Chem* 15: 1126–1146, 2008.

102. Nelson MT, Bonev AD. The β1 subunit of the Ca^{2+}-sensitive K^+ channel protects against hypertension. *J Clin Invest* 113: 955–957, 2004.

103. Nelson MT, Cheng H, Rubart M, Santana LF, Bonev AD, Knot HJ, Lederer WJ. Relaxation of arterial smooth muscle by calcium sparks. *Science* 270: 633–637, 1995.

104. Nelson RD, Kuan G, Saier MH Jr, Montal M. Modular assembly of voltage-gated channel proteins: a sequence analysis and phylogenetic study. *J Mol Microbiol Biotechnol* 1: 281–287, 1999.

105. Nimigean CM, Magleby KL. The beta subunit increases the Ca^{2+} sensitivity of large conductance Ca^{2+}-activated potassium channels by retaining the gating in the bursting states. *J Gen Physiol* 113: 425–440, 1999.

106. Niu X, Qian X, Magleby KL. Linker-gating ring complex as passive spring and Ca^{2+}-dependent machine for a voltage- and Ca^{2+}-activated potassium channel. *Neuron* 42: 745–756, 2004.

107. Orio P, Latorre R. Differential effects of β1 and β2 subunits on BK channel activity. *J Gen Physiol* 125: 395–411, 2005.

108. Orio P, Torres Y, Rojas P, Carvacho I, Garcia ML, Toro L, Valverde MA, Latorre R. Structural determinants for functional coupling between the β and α subunits in the Ca^{2+}-activated K^+ (BK) channel. *J Gen Physiol* 127: 191–204, 2006.

109. Pallotta BS. N-bromoacetamide removes a calcium-dependent component of channel opening from calcium-activated potassium channels in rat skeletal muscle. *J Gen Physiol* 86: 601–611, 1985.

110. Pallotta BS, Magleby KL, Barrett JN. Single channel recordings of Ca^{2+}-activated K^+ currents in rat muscle cell culture. *Nature* 293: 471–474, 1981.

111. Pantazis A, Gudzenko V, Savalli N, Sigg D, Olcese R. Operation of the voltage sensor of a human voltage- and Ca^{2+}-activated K^+ channel. *Proc Natl Acad Sci USA* 107: 4459–4464, 2010.

112. Pantazis A, Kohanteb AP, Olcese R. Relative motion of transmembrane segments S0 and S4 during voltage sensor activation in the human BK_{Ca} channel. *J Gen Physiol* 136: 645–657, 2010.

113. Pantazis A, Olcese R. Relative transmembrane segment rearrangements during BK channel activation resolved by structurally assigned fluorophore-quencher pairing. *J Gen Physiol* 140: 207–218, 2012.

114. Papazian DM, Shao XM, Seoh SA, Mock AF, Huang Y, Wainstock DH. Electrostatic interactions of S4 voltage sensor in Shaker K^+ channel. *Neuron* 14: 1293–1301, 1995.

115. Perez GJ, Bonev AD, Nelson MT. Micromolar Ca^{2+} from sparks activates Ca^{2+}-sensitive K^+ channels in rat cerebral artery smooth muscle. *Am J Physiol Cell Physiol* 281: C1769–C1775, 2001.

116. Permyakov EA. *Metalloproteomics*. Hoboken, NJ: John Wiley & Sons, 2009.

117. Petersen OH, Maruyama Y. Calcium-activated potassium channels and their role in secretion. *Nature* 307: 693–696, 1984.

118. Qian X, Nimigean CM, Niu X, Moss BL, Magleby KL. Slo1 tail domains, but not the Ca^{2+} bowl, are required for the β1 subunit to increase the apparent Ca^{2+} sensitivity of BK channels. *J Gen Physiol* 120: 829–843, 2002.

119. Qian X, Niu X, Magleby KL. Intra- and intersubunit cooperativity in activation of BK channels by Ca^{2+}. *J Gen Physiol* 128: 389–404, 2006.

120. Reinhart PH, Chung S, Levitan IB. A family of calcium-dependent potassium channels from rat brain. *Neuron* 2: 1031–1041, 1989.

121. Rothberg BS. Allosteric modulation of ion channels: the case of maxi-K. *Sci STKE*: pe16, 2004.

122. Rothberg BS, Magleby KL. Gating kinetics of single large-conductance Ca^{2+}-activated K^+ channels in high Ca^{2+} suggest a two-tiered allosteric gating mechanism. *J Gen Physiol* 114: 93–124, 1999.

123. Rothberg BS, Magleby KL. Voltage and Ca^{2+} activation of single large-conductance Ca^{2+}-activated K^+ channels described by a two-tiered allosteric gating mechanism. *J Gen Physiol* 116: 75–99, 2000.

124. Sadovsky E, Yifrach O. Principles underlying energetic coupling along an allosteric communication trajectory of a voltage-activated K^+ channel. *Proc Natl Acad Sci USA* 104: 19813–19818, 2007.

125. Sakai Y, Harvey M, Sokolowski B. Identification and quantification of full-length BK channel variants in the developing mouse cochlea. *J Neurosci Res* 89: 1747–1760, 2011.

126. Salazar H, Jara-Oseguera A, Hernandez-Garcia E, Llorente I, Arias O, II, Soriano-Garcia M, Islas LD, Rosenbaum T. Structural determinants of gating in the TRPV1 channel. *Nat Struct Mol Biol* 16: 704–710, 2009.

127. Salkoff L, Butler A, Ferreira G, Santi C, Wei A. High-conductance potassium channels of the SLO family. *Nat Rev Neurosci* 7: 921–931, 2006.

128. Santarelli LC, Chen J, Heinemann SH, Hoshi T. The β1 subunit enhances oxidative regulation of large-conductance calcium-activated K^+ channels. *J Gen Physiol* 124: 357–370, 2004.

129. Savalli N, Kondratiev A, de Quintana SB, Toro L, Olcese R. Modes of operation of the BK_{Ca} channel β2 subunit. *J Gen Physiol* 130: 117–131, 2007.

130. Savalli N, Pantazis A, Yusifov T, Sigg D, Olcese R. The contribution of RCK domains to human BK channel allosteric activation. *J Biol Chem* 287: 21741–21750, 2012.

131. Schoppa NE, Sigworth FJ. Activation of Shaker potassium channels III - an activation gating model for wild-type and V2 mutant channels. *J Gen Physiol* 111: 313–342, 1998.

132. Schopperle WM, Holmqvist MH, Zhou Y, Wang J, Wang Z, Griffith LC, Keselman I, Kusinitz F, Dagan D, Levitan IB. Slob, a novel protein that interacts with the Slowpoke calcium-dependent potassium channel. *Neuron* 20: 565–573, 1998.

133. Schreiber M, Salkoff L. A novel calcium-sensing domain in the BK channel. *Biophys J* 73: 1355–1363, 1997.

134. Schreiber M, Wei A, Yuan A, Gaut J, Saito M, Salkoff L. Slo3, a novel pH-sensitive K^+ channel from mammalian spermatocytes. *J Biol Chem* 273: 3509–3516, 1998.

135. Schubert R, Nelson MT. Protein kinases: tuners of the BK_{Ca} channel in smooth muscle. *Trends Pharmacol Sci* 22: 505–512, 2001.

136. Seibold MA, Wang B, Eng C, Kumar G, Beckman KB, Sen S, Choudhry S, Meade K, Lenoir M, Watson HG, Thyne S, Williams LK, Kumar R, Weiss KB, Grammer LC, Avila PC, Schleimer RP, Burchard EG, Brenner R. An African-specific functional polymorphism in KCNMB1 shows sex-specific association with asthma severity. *Hum Mol Genet*: 2681–2690, 2008.

137. Shao LR, Halvorsrud R, Borg-Graham L, Storm JF. The role of BK-type Ca^{2+}-dependent K^+ channels in spike broadening during repetitive firing in rat hippocampal pyramidal cells. *J Physiol* 521: 135–146, 1999.

138. Shen KZ, Lagrutta A, Davies NW, Standen NB, Adelman JP, North RA. Tetraethylammonium block of Slowpoke calcium-activated potassium channels expressed in *Xenopus* oocytes: evidence for tetrameric channel formation. *Pflügers Arch* 426: 440–445, 1994.

139. Shi J, Cui J. Intracellular Mg^{2+} enhances the function of BK-type Ca^{2+}-activated K^+ channels. *J Gen Physiol* 118: 589–606, 2001.

140. Shi J, Krishnamoorthy G, Yang Y, Hu L, Chaturvedi N, Harilal D, Qin J, Cui J. Mechanism of magnesium activation of calcium-activated potassium channels. *Nature* 418: 876–880, 2002.

141. Shipston MJ. Alternative splicing of potassium channels: a dynamic switch of cellular excitability. *Trends Cell Biol* 11: 353–358, 2001.

142. Sigg D. A linkage analysis toolkit for studying allosteric networks in ion channels. *J Gen Physiol* 141: 29–60, 2013.

143. Song L, Magleby KL. Testing for microscopic reversibility in the gating of maxi K^+ channels using two-dimensional dwell-time distributions. *Biophys J* 67: 91–104, 1994.

144. Stefani E, Ottolia M, Noceti F, Olcese R, Wallner M, Latorre R, Toro L. Voltage-controlled gating in a large conductance Ca^{2+}-sensitive K^+ channel (hslo). *Proc Natl Acad Sci USA* 94: 5427–5431, 1997.

145. Swartz KJ. Sensing voltage across lipid membranes. *Nature* 456: 891–897, 2008.

146. Sweet TB, Cox DH. Measurements of the BK_{Ca} channel's high-affinity Ca^{2+} binding constants: effects of membrane voltage. *J Gen Physiol* 132: 491–505, 2008.

147. Sweet TB, Cox DH. Measuring the influence of the BK_{Ca} β1 subunit on Ca^{2+} binding to the BK_{Ca} channel. *J Gen Physiol* 133: 139–150, 2009.

148. Tanaka Y, Meera P, Song M, Knaus HG, Toro L. Molecular constituents of maxi K_{Ca} channels in human coronary smooth muscle: predominant α + β subunit complexes. *J Physiol* 502: 545–557, 1997.

149. Tang QY, Zhang Z, Xia XM, Lingle CJ. Block of mouse Slo1 and Slo3 K^+ channels by CTX, IbTX, TEA, 4-AP and quinidine. *Channels (Austin)* 4: 22–41, 2010.

150. Tang XD, Xu R, Reynolds MF, Garcia ML, Heinemann SH, Hoshi T. Haem can bind to and inhibit mammalian calcium-dependent Slo1 BK channels. *Nature* 425: 531–535, 2003.

151. Tao X, Lee A, Limapichat W, Dougherty DA, MacKinnon R. A gating charge transfer center in voltage sensors. *Science* 328: 67–73, 2010.

152. Thompson J, Begenisich T. Selectivity filter gating in large-conductance Ca^{2+}-activated K^+ channels. *J Gen Physiol* 139: 235–244, 2012.

153. Thurm H, Fakler B, Oliver D. Ca^{2+}-independent activation of BK_{Ca} channels at negative potentials in mammalian inner hair cells. *J Physiol* 569: 137–151, 2005.

154. Tombola F, Pathak MM, Isacoff EY. How does voltage open an ion channel? *Annu Rev Cell Dev Biol* 22: 23–52, 2006.

155. Tricarico D, Mele A, Conte Camerino D. Phenotype-dependent functional and pharmacological properties of BK channels in skeletal muscle: effects of microgravity. *Neurobiol Dis* 20: 296–302, 2005.

156. Uebele VN, Lagrutta A, Wade T, Figueroa DJ, Liu Y, McKenna E, Austin CP, Bennett PB, Swanson R. Cloning and functional expression of two families of β-subunits of the large conductance calcium-activated K^+ channel. *J Biol Chem* 275: 23211–23218, 2000.

157. Vaithianathan T, Bukiya A, Liu J, Liu P, Asuncion-Chin M, Fan Z, Dopico A. Direct regulation of BK channels by phosphatidylinositol 4,5-bisphosphate as a novel signaling pathway. *J Gen Physiol* 132: 13–28, 2008.

158. Valverde MA, Rojas P, Amigo J, Cosmelli D, Orio P, Bahamonde MI, Mann GE, Vergara C, Latorre R. Acute activation of Maxi-K channels (hSlo) by estradiol binding to the β subunit. *Science* 285: 1929–1931, 1999.

159. Vargas E, Bezanilla F, Roux B. In search of a consensus model of the resting state of a voltage-sensing domain. *Neuron* 72: 713–720, 2011.

160. Wallner M, Meera P, Toro L. Determinant for beta-subunit regulation in high-conductance voltage-activated and Ca^{2+}-sensitive K^+ channels: an additional transmembrane region at the N terminus. *Proc Natl Acad Sci USA* 93: 14922–14927, 1996.

161. Wallner M, Meera P, Toro L. Molecular basis of fast inactivation in voltage and Ca^{2+}-activated K^+ channels: a transmembrane beta-subunit homolog. *Proc Natl Acad Sci USA* 96: 4137–4142, 1999.

162. Wang B, Rothberg BS, Brenner R. Mechanism of β4 subunit modulation of BK channels. *J Gen Physiol* 127: 449–465, 2006.

163. Wang L, Sigworth FJ. Structure of the BK potassium channel in a lipid membrane from electron cryomicroscopy. *Nature* 461: 292–295, 2009.

164. Wang YW, Ding JP, Xia XM, Lingle CJ. Consequences of the stoichiometry of Slo1 α and auxiliary β subunits on functional properties of large-conductance Ca^{2+}-activated K^+ channels. *J Neurosci* 22: 1550–1561, 2002.

165. Weiger TM, Holmqvist MH, Levitan IB, Clark FT, Sprague S, Huang WJ, Ge P, Wang C, Lawson D, Jurman ME, Glucksmann MA, Silos-Santiago I, DiStefano PS, Curtis R. A novel nervous system beta subunit that downregulates human large conductance calcium-dependent potassium channels. *J Neurosci* 20: 3563–3570, 2000.

166. Werner ME, Zvara P, Meredith AL, Aldrich RW, Nelson MT. Erectile dysfunction in mice lacking the large-conductance calcium-activated potassium (BK) channel. *J Physiol* 567: 545–556, 2005.

167. Wilkens CM, Aldrich RW. State-independent block of BK channels by an intracellular quaternary ammonium. *J Gen Physiol* 128: 347–364, 2006.

168. Wu RS, Chudasama N, Zakharov SI, Doshi D, Motoike H, Liu G, Yao Y, Niu X, Deng SX, Landry DW, Karlin A, Marx SO. Location of the β4 transmembrane helices in the BK potassium channel. *J Neurosci* 29: 8321–8328, 2009.

169. Wu RS, Liu G, Zakharov SI, Chudasama N, Motoike H, Karlin A, Marx SO. Positions of β2 and β3 subunits in the large-conductance calcium- and voltage-activated BK potassium channel. *J Gen Physiol* 141: 105–117, 2013.

170. Wu RS, Marx SO. The BK potassium channel in the vascular smooth muscle and kidney: α- and β-subunits. *Kidney Int* 78: 963–974, 2010.

171. Wu Y, Xiong Y, Wang S, Yi H, Li H, Pan N, Horrigan FT, Ding J. Intersubunit coupling in the pore of BK channels. *J Biol Chem* 284: 23353–23363, 2009.

172. Wu Y, Yang Y, Ye S, Jiang Y. Structure of the gating ring from the human large-conductance Ca^{2+}-gated K^+ channel. *Nature* 466: 393–397, 2010.

173. Xia XM, Ding JP, Lingle CJ. Molecular basis for the inactivation of Ca^{2+}- and voltage-dependent BK channels in adrenal chromaffin cells and rat insulinoma tumor cells. *J Neurosci* 19: 5255–5264, 1999.

174. Xia XM, Ding JP, Zeng XH, Duan KL, Lingle CJ. Rectification and rapid activation at low Ca^{2+} of Ca^{2+}-activated, voltage-dependent BK currents: consequences of rapid inactivation by a novel β subunit. *J Neurosci* 20: 4890–4903, 2000.

175. Xia XM, Zeng X, Lingle CJ. Multiple regulatory sites in large-conductance calcium-activated potassium channels. *Nature* 418: 880–884, 2002.

176. Yan J, Aldrich RW. BK potassium channel modulation by leucine-rich repeat-containing proteins. *Proc Natl Acad Sci USA* 109: 7917–7922, 2012.

177. Yan J, Aldrich RW. LRRC26 auxiliary protein allows BK channel activation at resting voltage without calcium. *Nature* 466: 513–516, 2010.

178. Yang C, Zeng XH, Zhou Y, Xia XM, Lingle CJ. LRRC52 (leucine-rich-repeat-containing protein 52), a testis-specific auxiliary subunit of the alkalization-activated Slo3 channel. *Proc Natl Acad Sci USA* 108: 19419–19424, 2011.

179. Yang H, Hu L, Shi J, Cui J. Tuning magnesium sensitivity of BK channels by mutations. *Biophys J* 91: 2892–2900, 2006.

180. Yang H, Hu L, Shi J, Delaloye K, Horrigan FT, Cui J. Mg^{2+} mediates interaction between the voltage sensor and cytosolic domain to activate BK channels. *Proc Natl Acad Sci USA* 104: 18270–18275, 2007.

181. Yang H, Shi J, Zhang G, Yang J, Delaloye K, Cui J. Activation of Slo1 BK channels by Mg^{2+} coordinated between the voltage sensor and RCK1 domains. *Nat Struct Mol Biol* 15: 1152–1159, 2008.

182. Yang H, Zhang G, Shi J, Lee US, Delaloye K, Cui J. Subunit-specific effect of the voltage sensor domain on Ca^{2+} sensitivity of BK channels. *Biophys J* 94: 4678–4687, 2008.

183. Yuan P, Leonetti MD, Hsiung Y, MacKinnon R. Open structure of the Ca^{2+} gating ring in the high-conductance Ca^{2+}-activated K^{+} channel. *Nature* 481: 94–97, 2012.

184. Yuan P, Leonetti MD, Pico AR, Hsiung Y, Mackinnon R. Structure of the human BK channel Ca^{2+}-activation apparatus at 3.0 Å resolution. *Science* 329: 182–186, 2010.

185. Yusifov T, Javaherian AD, Pantazis A, Gandhi CS, Olcese R. The RCK1 domain of the human BK_{Ca} channel transduces Ca^{2+} binding into structural rearrangements. *J Gen Physiol* 136: 189–202, 2010.

186. Yusifov T, Savalli N, Gandhi CS, Ottolia M, Olcese R. The RCK2 domain of the human BK_{Ca} channel is a calcium sensor. *Proc Natl Acad Sci USA* 105: 376–381, 2008.

187. Zagotta WN, Hoshi T, Aldrich RW. Shaker potassium channel gating. III: Evaluation of kinetic models for activation. *J Gen Physiol* 103: 321–362, 1994.

188. Zeng XH, Ding JP, Xia XM, Lingle CJ. Gating properties conferred on BK channels by the beta3b auxiliary subunit in the absence of its NH_2- and COOH termini. *J Gen Physiol* 117: 607–628, 2001.

189. Zeng XH, Xia XM, Lingle CJ. Divalent cation sensitivity of BK channel activation supports the existence of three distinct binding sites. *J Gen Physiol* 125: 273–286, 2005.

190. Zhang G, Huang SY, Yang J, Shi J, Yang X, Moller A, Zou X, Cui J. Ion sensing in the RCK1 domain of BK channels. *Proc Natl Acad Sci USA* 107: 18700–18705, 2010.

191. Zhang X, Solaro CR, Lingle CJ. Allosteric regulation of BK channel gating by Ca^{2+} and Mg^{2+} through a nonselective, low affinity divalent cation site. *J Gen Physiol* 118: 607–635, 2001.

192. Zhang Y, Gao YJ, Zuo J, Lee RM, Janssen LJ. Alteration of arterial smooth muscle potassium channel composition and BK_{Ca} current modulation in hypertension. *Eur J Pharmacol* 514: 111–119, 2005.

193. Zhao G, Neeb ZP, Leo MD, Pachuau J, Adebiyi A, Ouyang K, Chen J, Jaggar JH. Type 1 IP3 receptors activate BK_{Ca} channels via local molecular coupling in arterial smooth muscle cells. *J Gen Physiol* 136: 283–291, 2010.

194. Zhou Y, Xia XM, Lingle CJ. Cysteine scanning and modification reveal major differences between BK channels and Kv channels in the inner pore region. *Proc Natl Acad Sci USA* 108: 12161–12166, 2011.

195. Zhou Y, Zeng XH, Lingle CJ. Barium ions selectively activate BK channels via the Ca^{2+}-bowl site. *Proc Natl Acad Sci USA* 109: 11413–11418, 2012.

196. ZhuGe R, Fogarty KE, Tuft RA, Walsh JV Jr. Spontaneous transient outward currents arise from microdomains where BK channels are exposed to a mean Ca^{2+} concentration on the order of 10 microM during a Ca^{2+} spark. *J Gen Physiol* 120: 15–27, 2002.

197. Zweifach A, Lewis RS. Rapid inactivation of depletion-activated calcium current (ICRAC) due to local calcium feedback. *J Gen Physiol* 105: 209–226, 1995.